ARTI-21CR/611-10060-01

CO_2 COMPRESSOR-EXPANDER ANALYSIS

Final Report

Date Published – March 2003

Hans-Joachim Huff, Reinhard Radermacher

CEEE
Department of Mechanical Engineering
University of Maryland
College park, MD 20742-3035
(301) 405 5286
raderm@umd.edu

Prepared for the
AIR-CONDITIONING AND REFRIGERATION TECHNOLOGY INSTITUTE
4100 N. Fairfax Drive, Suite 200, Arlington, Virginia 22203

DISCLAIMER

This report was prepared as an account of work sponsored by the Air-Conditioning and Refrigeration Technology Institute (ARTI) under its "HVAC&R Research for the 21st Century" (21-CR) program. Neither ARTI, the financial supporters of the 21-CR program, or any agency thereof, nor any of their employees, contractors, subcontractors or employees thereof - makes any warranty, expressed or implied; assumes any legal liability or responsibility for the accuracy, completeness, any third party's use of, or the results of such use of any information, apparatus, product, or process disclosed in this report; or represents that its use would not infringe privately owned rights. Reference herein to any specific commercial product, process, or service by trade name, trademark, manufacturer, or otherwise, does not necessarily constitute nor imply its endorsement, recommendation, or favoring by ARTI, its sponsors, or any agency thereof or their contractors or subcontractors. The views and opinions of authors expressed herein do not necessarily state or reflect those of ARTI, the 21-CR program sponsors, or any agency thereof.

Funding for the 21-CR program provided by (listed in order of support magnitude):
- U.S. Department of Energy (DOE Cooperative Agreement No. DE-FC05-99OR22674)
- Air-Conditioning & Refrigeration Institute (ARI)
- Copper Development Association (CDA)
- New York State Energy Research and Development Authority (NYSERDA)
- California Energy Commission (CEC)
- Refrigeration Service Engineers Society (RSES)
- Heating, Refrigeration and Air Conditioning Institute of Canada (HRAI)

Available to the public from

U.S. Department of Commerce
National Technical Information Service
5285 Port Royal Road
Springfield, VA 22161
(703) 487-4650

Available to U.S. Department of Energy and its contractors in paper from

U.S. Department of Energy
Office of Scientific and Technical Information
P.O. Box 62
Oak Ridge, TN 37831
(423) 576-8401

ARTI-21CR/611-10060-01

CO_2 COMPRESSOR-EXPANDER ANALYSIS
Final Report

Date Published – March 2003

Hans-Joachim Huff, Reinhard Radermacher

Prepared for the
AIR-CONDITIONING AND REFRIGERATION TECHNOLOGY INSTITUTE
Under ARTI 21-CR Program Contract Number 611-10060

EXECUTIVE SUMMARY

Background

Carbon dioxide (CO_2) is a potential substitute for HCFC refrigerants with favorable environmental properties compared to other HCFC alternatives. One of the major challenges with CO_2 in air-conditioning applications is the low energy efficiency of systems at higher heat sink temperatures . The major loss in CO_2 cycles is the throttling loss associated with the expansion process. The availability lost during the expansion process can be recovered with a work-producing expansion device, an expander. Theoretical studies have estimated improvements of the basic CO_2 cycle in the range of 40% to 60% for outdoor temperatures of 27°C to 50°C, resulting in efficiencies competitive with or better than those of current conventional systems.

Objective

The overall objective of this project is to provide the HVAC industry with elements to understand the practical performance potential of CO_2 as an alternate refrigerant in residential air-conditioning applications through the implementation of an expander – compressor system. The work analytically defines the most promising approaches from a performance and feasibility standpoint. The work accounts for the requirements inherent in the integration of the selected types of expanders into CO_2 systems, in order to provide a realistic evaluation of the system performance.

System Performance with Expander, CO_2 vs. R22

The energy efficiency of a CO_2 air-conditioning system with conventional expansion valve and without suction line heat exchanger at an outdoor air temperature of 28°C is approximately 4% to 6% lower than the energy efficiency of a comparable R22 system. At outdoor air temperatures of 50°C, the energy efficiency of the CO_2 system is approximately 43% lower. A CO_2 system with an ideal expander performs 25% to 38% more efficiently at 28°C than an R22 system with a conventional expansion valve. At 50°C, the ideal CO_2 expander system is 4% to 7% more efficient than the R22 system. If the expander efficiency is 80%, the CO_2 system performs 16% to 27% better than the R22 system at 28°C and 7% to 11% worse at 50°C. At approximately 36°C, both systems perform with a similar efficiency. With an expander of 60% efficiency, the CO_2 system performs 7% to 18% better at 28°C and 18% to 21% worse at 50°C. At approximately 31°C, the performance of both systems is equal. If the expansion valve is replaced by an ideal work-recovering expander in both systems, the CO_2 system performs 19% to 31% more energy efficiently at outdoor air temperatures of 28°C. At 50°C, the CO_2 system performs approximately 9% to 12% worse than the R22 system. With an expander efficiency of 80%, the CO_2 system performs 10% to 21% better at 28°C and 19% to 22% worse at 50°C. If the efficiency of the expander is 60%, the energy efficiency of the CO_2 system is 4% to 14% higher than the R22 system at 28°C and 26% to 29% lower at 50°C

outdoor air temperature. Table A lists the estimated coefficient of performance for the systems.

Table A: COP of CO_2 and R22 systems at ambient temperatures of 28°C and 50°C:

Expander efficiency [%]	28°C		50°C	
	CO_2	R22	CO_2	R22
100	6.9 – 7.6	5.8	2.9 - 3	3.3
80	6.4 – 7.0	5.8	2.5 – 2.6	3.2
60	5.9 – 6.5	5.7	2.2 – 2.3	3.1
0	4.8 – 5.3	5.5	1.6	2.8

Effect of Suction Line Heat Exchanger in Expander System

At most operating conditions, a suction line heat exchanger does not improve the energy efficiency of an expander system. Only if a significant fraction (more than 70%) of the work extracted from the expansion process is lost during the energy conversion does the performance benefit from an internal heat exchanger. If more than 30% of the expander work can be recovered, the suction line heat exchanger reduces the energy efficiency of the system. This is due to the reduced work output at lower expander inlet enthalpy and the increased compressor work at higher super-heat. However, it should be noted that a suction line heat exchanger can have secondary benefits, such as protection of the compressor at operation with flooded evaporator, and should not be excluded from the system without careful consideration.

Expander and Compressor Performance

Three positive displacement mechanisms have been analyzed for their potential as expansion machines in a CO_2 system:

(1) Reciprocating piston
(2) Rotary piston
(3) Scroll

Tables B and C summarize the expected performance for the devices as compressors and expanders at AHSRAE A test conditions for a range of machining tolerances (leakage gap size).

Table B: Compressor indicated, isentropic, and volumetric efficiency vs. leakage gap size

	5 µm			10 µm			15 µm		
	η_{ind}	η_{is}	η_{vol}	η_{ind}	η_{is}	η_{vol}	η_{ind}	η_{is}	η_{vol}
Recip. piston	0.93	0.77	0.88	0.91	0.76	0.84	0.85	0.72	0.79
Rotary piston	0.96	0.79	0.96	0.90	0.75	0.92	0.85	0.72	0.87
Scroll	0.87	0.73	0.88	0.64	0.56	0.65	0.39	0.36	0.38

Table C: Expander indicated and isentropic efficiency vs. leakage gap size

	5 μm		10 μm		15 μm	
	η_{ind}	η_{is}	η_{ind}	η_{is}	η_{ind}	η_{is}
Recip. piston	0.90	0.75	0.87	0.72	0.81	0.66
Rotary piston	0.94	0.79	0.84	0.69	0.78	0.63
Scroll	0.93	0.78	0.75	0.60	0.47	0.32

The performance of the scroll mechanism is most dependent on the leakage gap size. At machining tolerances above 5 μm, the scroll mechanism performs significantly worse than the other mechanisms. The performance of the scroll mechanism is dominated by the leakage across the tips of the scroll wraps. If this leakage path is eliminated, the indicated efficiency of a scroll expander, for instance, is above 90% for a flank clearance of 15 μm. Experimental results of existing scroll compressors for conventional refrigerants show a high volumetric and compression efficiency, indicating that effective techniques for leakage reduction are available. The reciprocating piston and rotary piston mechanisms perform similarly at all leakage clearances. At small leakage gap sizes, the rotary piston performs slightly better than the reciprocating piston.

The reciprocating and rotary piston expanders require externally actuated valves. With externally activated and controlled valves, current technology limits the expander frequency to values on the order of 1 Hz. The scroll mechanism is not subject to this limitation. All mechanisms require some kind of valve controls to adjust the volume ratio. If the inlet valves of an expander are not controlled, the internal volume ratio is constant. If the internal volume ratio does not match the ideal volume ratio imposed by the operating conditions, over- or under-expansion reduces the expander efficiency. Performance simulation indicates that the ideal volume ratio in a CO_2 system with optimized high-side pressure changes by less than 25% over a wide range of operating conditions. The expander performance degradation due to over- or under-expansion is below 10%, indicating that expander valve control may not be necessary.

Due to the small change of the pressure ratio over a wide range of operating conditions in a CO_2 system, the compressor and expander indicated efficiencies are approximately constant at all operating conditions. The indicated efficiencies of a reciprocating piston compressor and a reciprocating piston expander with a leakage gap size of 10 μm are approximately 91% and 87%, respectively. With an effective isentropic efficiency 15% lower than the indicated efficiency (i.e. 76% and 72% for compressor and expander, respectively), the COP of an optimized CO_2 expander system is approximately 6.6 at 28°C outdoor air temperature and 2.4 at 50°C. Compared to a conventional R22 system, the CO_2 expander system performs 20% better at the low temperature conditions and approximately 14% worse at the high-temperature conditions. At approximately 34°C, both systems operate with the same energy efficiency.

Integration Concepts

For maximum efficiency, the mechanical work generated by the expander should be directly utilized. To reduce conversion and storage losses, the expander work can supply

part of the compressor shaft work, requiring the integration of the compressor and expander on a common shaft. With this design however, the optimization of the high-side pressure becomes a challenge, because the high-side pressure is no longer independent from the compressor speed (unless the expander displacement volume is variable). A number of control options have been analyzed. System simulations indicate that an expander cycle can be operated at or close to the optimum high-side pressure without variable expander displacement or additional control valves if the compressor and expander displacement volumes are designed appropriately.

TABLE OF CONTENTS

LIST OF FIGURES

LIST OF TABLES

LIST OF SYMBOLS

Latin Symbols

Symbol		Unit
A	Area	m^2
C_d	Discharge coefficient	
COP	Coefficient of performance	
d_h	Hydraulic diameter	m
F	Field	
h	Specific enthalpy	kJ/kg
$\dot{H}$	Enthalpy flow rate	kJ/s
k_m	Coefficient for minor losses	
m	mass	kg
$\dot{m}$	Mass flow rate	kg/s
Nu	Nusselt number	
P	Pressure	kPa
pr	Pressure ratio	
Q	Heat	kJ
$\dot{Q}$	Heat flow rate	kW
q	Specific heat	kJ/kg
R, r	Gas constant, Radius	kJ/kg·K, m
Re	Reynolds number	
r_d	Ratio of vapor density to liquid density	
Ref	Refrigerant	
S	Entropy	kJ/K
s	Specific entropy	kJ/kg·K
$\dot{S}$	Entropy flow rate	kW/K
T	Temperature	°C, K
TDC	Top dead center, position of piston stop	
U,u	Absolute, specific internal energy	kJ, kJ/kg
v	Velocity	m/s
V	Volume	m^3
w	Specific work	kJ/kg
$\dot{W}$	Power	kW
x	Vapor quality	
y	Entropy generation contribution	

Greek Symbols

β	Mismatch of volume ratio, volumetric expansion coefficient, velocity of approach factor	- / K^{-1}
γ	Isentropic expansion exponent	
δ	Leakage gap size	m
θ	Corrective coefficient for 2-phase orifice flow	

μ	Joule-Thomson coefficient, viscosity	kg/m^3, kg/m·s

Subscripts and Superscripts

*	Intermediate state
C	Cooling
Comp	Compressor
Cond	Condenser
D	Discharge
Evap	Evaporator
Exp	Expansion, expander, expansion valve
G	Gas phase
GC	Gas cooler
is	Isentropic reversible process
j	Iteration index
L	Liquid phase
Leak	Associated with leak flow
Q	Associated with heat transfer
up	Upstream
Valve	Associated with valve flow

1 INTRODUCTION

Background

Carbon dioxide (CO_2) is a potential substitute for HCFC refrigerants with favorable environmental properties compared to other HCFC alternatives. One of the major challenges with CO_2 in air-conditioning applications is the low system energy efficiency at higher heat sink temperatures. The major loss in CO_2 cycles is the throttling loss associated with the expansion process. The availability lost during the expansion process can be recovered with a work-producing expansion device (expander). Theoretical studies have estimated improvements of the basic CO_2 cycle in the range of 40% to 60% for outdoor temperatures of 27°C to 50°C, resulting in efficiencies competitive with or better than those of current conventional system.

Objective

The overall objective of this project is to provide the HVAC industry with elements to understand the practical performance potential of CO_2 as an alternate refrigerant in residential air-conditioning applications through the implementation of an expander – compressor system. The work analytically defines the most promising approaches from a performance and feasibility standpoint. The work accounts for the requirements inherent in the integration of the selected types of expanders into CO_2 systems, in order to provide a realistic evaluation of the performance.

Overview

Following the definition of a baseline and review of the recent literature on CO_2 vapor compression systems with and without expanders, the performance potential of a CO_2 expander system depending on the expander efficiency is estimated and compared to a conventional, sub-critical system with and without expander. Section 5 presents the approach for the simulation of the compressor and expander efficiency in a CO_2 system. Results of the simulation for four compressor and expander mechanisms are presented and compared in Section 6. The potential for the compressor – expander integration and implications for the cycle control are discussed in Section 7. Section 8 summarizes and concludes the report.

2 BASELINE OF CONVENTIONAL AIR-CONDITIONING SYSTEMS

The baseline for the performance evaluation of the CO_2 transcritical vapor compression cycle is a 10 kW residential air-conditioning system with refrigerant R22. Extensive laboratory and field data is available to the industry, thus an experimental baseline is not established here. For the comparison between the CO_2 system and the R22 system, a simplified model is created. The modeling assumptions are given in Appendix A. The R22 and CO_2 systems with and without expander are briefly compared in Section 4.

3 REVIEW OF RECENT WORK ON CO_2 SYSTEMS

3.1 CO_2 Baseline Systems

The primary target application for transcritical CO_2 vapor compression system has been automotive air-conditioning. Consequently, most of the research has focused on automotive applications (e.g. Preissner 2001, Adiprasito 2000, Hirao et al. 2000, Ijima 2000, McEnaney et al. 1998). Work on residential size systems has been published among others by Cuttler (2000), Halozan and Rieberer (1999), Heyl (2000), Hwang and Radermacher (1998a), Neksa et al. (1998) and Rieberer et al. (1999).

For the comparison with a residential air-conditioning system, the work by Cuttler (2000) is the most appropriate option. The focus of Cuttler's work was to develop and experimentally investigate a CO_2 air-conditioning system to replace a 12 kW environmental control unit with R22 as refrigerant. Experimental data are available at the CEEE of the University of Maryland. The system performance at ASHRAE A, B, and C test conditions is shown in Table 1.

Table 1: Performance data of 12 kW CO_2 air-conditioning system (Cuttler 2000)

	ASHRAE A	ASHRAE B	ASHRAE C
COP	2.9	3.5	3.4
Cooling capacity [kW]	12	12.2	11.6

3.2 Work Recovery Devices and Cycles with Work Recovery

Shortly after interest in CO_2 cycles was reinvigorated in the early 1990s, the expansion valve was identified as a major source of exergy loss and the use of work recovery machines began to be reconsidered theoretically (Lorentzen 1994 and later Robinson and Groll 1998, Heyl and Quack 2000, Preissner 2001, Fukuta et al. 2001). Depending on modeling assumptions, the researchers estimate the potential for improvement of energy efficiency to be 20% to 50%.

Heyl and Quack (2000) conducted experiments with a reciprocating piston expander and reported an isentropic efficiency of 51%. They investigated a system with two-stage compression where the second compressor stage was driven by the piston expander. The COP of the set-up was 30% higher than the COP of the two-stage system without expander. Maurer and Zinn (2000) conducted experiments with reciprocating piston type devices and gear pump type devices. The isentropic efficiency of the piston expander and the gear pump device were on the order of 50% and 55%, respectively. The energy efficiency of the refrigeration cycle was not measured. Preissner (2001) performed experiments with a modified R134a scroll compressor operating as an expander. Due to high internal leakage, the isentropic efficiency was lower than 30%. The advantage of scroll expanders pointed out by Preissner is the built-in volume ratio of the device. While piston expanders require active valves, the timing of suction and discharge in scroll expanders is purely determined be the geometry of the device. This reduces the level of

control complexity and still allows a large portion of the volume change work of the expansion process to be used. A reciprocating piston expander was built and tested by Baek et al. (2002). The measured isentropic efficiency was less than 10% and the improvement of the system COP was on the order of 10%. The system set-up was similar to that of Heyl and Quack (2000). Stosic et al. (2002) report test results from a twin screw combined compressor and expander in a low-temperature application for CO_2. The isentropic efficiency of the expander section was on the order of 65%. The system was operated below the critical point. Similar to scroll expanders, screw devices have a built-in volume ratio and thus do not require control valves.

3.3 Other Cycle Improvements

In most of the investigations referenced in Section 3.1, the CO_2 cycles were equipped with a suction line heat exchanger (SLHX), which accommodates internal heat transfer between gas cooler outlet and evaporator outlet. The effect of an SLHX is more pronounced at high temperatures of the heat sink (Preissner 2001). Preissner observed an improvement of the COP of 13% and of the capacity of 18% at gas cooler air inlet temperatures of 45°C and an insignificant effect on the performance at temperatures of 15°C.

Nippon Soken and Denso Corporation (1997) and Huff et al. (2002) investigated the potential for performance improvement by employing a two-stage compression process. They explored various options for the circuitry and reported a COP improvement in the order of 20% to 60% and an increase in cooling capacity of 10% to 35% for the most promising option. In addition to the basic components of a heat pump cycle and the modified compressor, this two-stage system requires two internal heat exchangers and one additional secondary fluid – refrigerant heat exchanger.

At the Center for Environmental Energy Engineering (CEEE) of the University of Maryland, the benefit of an evaporatively cooled gas cooler has been investigated (Preissner 2001, Preissner et al. 2000). Using liquid water drained from the evaporator, the air at the gas cooler inlet can be humidified and thereby cooled. A theoretical performance improvement of 40% in COP and capacity is predicted. In preliminary experiments, the COP improvement was 24% and the capacity increased by 8%. Problems encountered in the experiments included uneven distribution of the water over the gas cooler and incomplete evaporation. The power required for driving the pump, which was used to spray the water into the air-stream, was not included into the net work-input to the system.

4 PERFORMANCE POTENTIAL OF CO_2 EXPANDER SYSTEMS

Figure 1 shows the difference between a cycle with isenthalpic and isentropic expansion in a P-h diagram for CO_2. The cycle with isentropic expansion operates between the points 1 – 2 – 3 – 4 and the cycle with isenthalpic expansion between the points 1 – 2 – 3 – 4′.

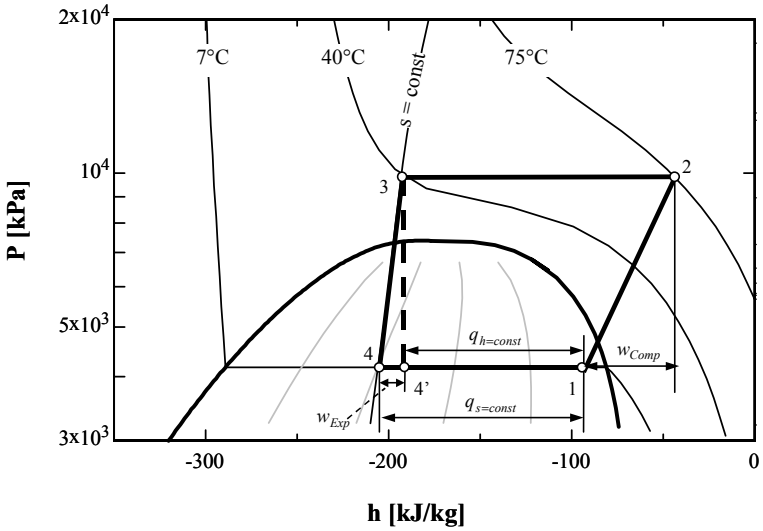

Figure 1: Transcritical CO_2 cycle with isenthalpic and isentropic expansion

In order for the expansion process to follow a line of constant entropy, the enthalpy difference $h_{4'} - h_4$ must be extracted in the form of expansion work. This means that the cycle with isentropic expansion must have a work-extracting expansion device. The work produced can reduce the net work-input to the cycle. At the same time, the capacity of the cycle is increased by the difference $h_{4'} - h_4$. Thus, the isentropic expansion reduces the net work-input to the cycle and increases the capacity.

An isentropic expansion process is technically impossible due to friction, leakage, and other unavoidable sources of irreversibility. In realistic applications, the process in a work-extracting expansion device, commonly referred to as an expander, will instead be a polytropic one, resulting in an evaporator inlet state between point 4 and 4′ in Figure 1. The real process in an expander compared to the ideal isentropic process is usually characterized by the expander isentropic efficiency η_{is}^{Exp}

$$\eta_{is}^{Exp} = \frac{h(P_i, s_i) - h(P_o, s_o)}{h(P_i, s_i) - h(P_o, s_i)} = \frac{W_{real}^{Exp}}{W_{is}^{Exp}} \quad \text{Equation 1}$$

Similar to the isentropic efficiency of a compressor, this definition is only applicable if the process can be considered adiabatic. The isenthalpic throttling valve can be considered as an expander with isentropic efficiency of zero.

A first-law analysis allows estimating the potential for system performance improvement using an expander. The analysis has been carried out for both a transcritical CO_2 cycle and a subcritical R22 system. It is assumed that all of the work from the expansion process is recovered and contributes to the total system work-input. Detailed modeling assumptions are given in Appendix A.

Figure 2 graphs the result of the simulation over a range of ambient temperatures between 28°C and 50°C and expander efficiencies between 0% and 100%. Without expander, the R22 system performs better than or equal to the CO_2 system at all ambient temperatures (Figure 2 a). A CO_2 system with isentropic expansion performs better than the baseline R22 system with conventional expansion valve over the range of ambient temperatures considered. With an isentropic expander in both cycles, the CO_2 system performs better than the R22 system at ambient temperatures below 38°C (Figure 2 b).

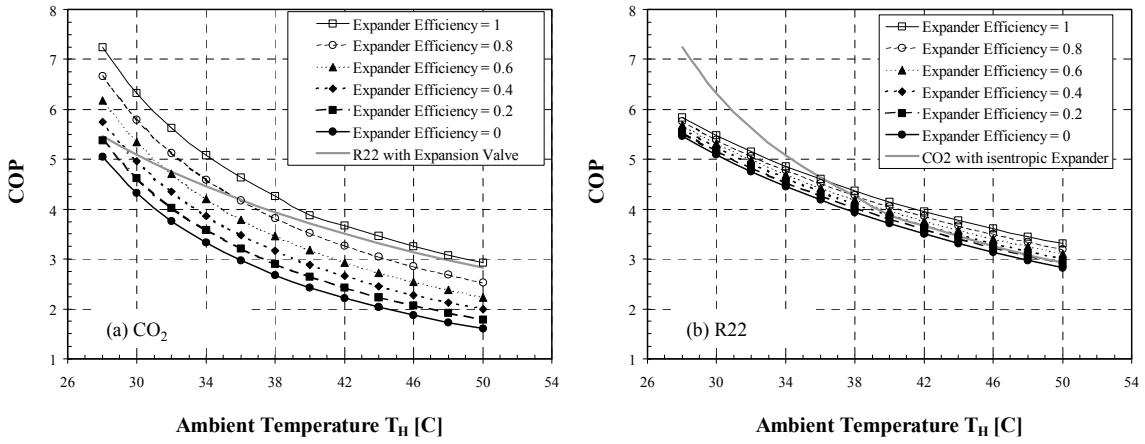

Figure 2: Performance potential of expander cycle for refrigerants CO_2 (a) and R22 (b)

Expander and Suction Line Heat Exchanger

A suction line heat exchanger (SLHX) is a refrigerant to refrigerant heat exchanger, accommodating internal heat transfer between compressor suction line and gas cooler/condenser outlet. For CO_2 systems with isenthalpic expansion valves, an SLHX can improve the performance by up to 15% at high ambient temperatures. An SLHX is considered an integral component in these systems. In cycles with work-extracting expansion however, an SLHX does not always improve the system performance. An SLHX can be characterized by its effectiveness

$$\varepsilon_{SLHX} = \frac{h\left(T_{low,out}, P_{low,out}\right) - h\left(T_{low,in}, P_{low,in}\right)}{h\left(T_{high,in}, P_{low,out}\right) - h\left(T_{low,in}, P_{low,in}\right)}, \qquad \text{Equation 2}$$

where *in* and *out* refer to the inlet and outlet of the SLHX and *low* and *high* refer to the low-pressure and high-pressure sides, respectively.

The energy efficiency improvement of an SLHX depends on whether the work extracted in the expander can be recovered. If the expander work is not utilized to reduce the net-work input to the system, the expansion process can still follow a line of constant entropy, improving the cooling capacity. However, the COP would be significantly smaller compared to the case with perfect work recovery.

Figure 3 shows the performance of four different cycle configurations over a range of ambient temperatures. Graph (a) presents the system with work recovery, graph (b) the system without work recovery. An isentropic efficiency η_{Exp}=0 indicates a system without expander, η_{Exp}=1 represents an isentropic expander. An SLHX effectiveness ε_{SLHX}=1 indicates a system with ideal SLHX. The system without SLHX is represented by ε_{SLHX}=0. No pressure drop in the SLHX is considered; thus the results represent a best-case scenario.

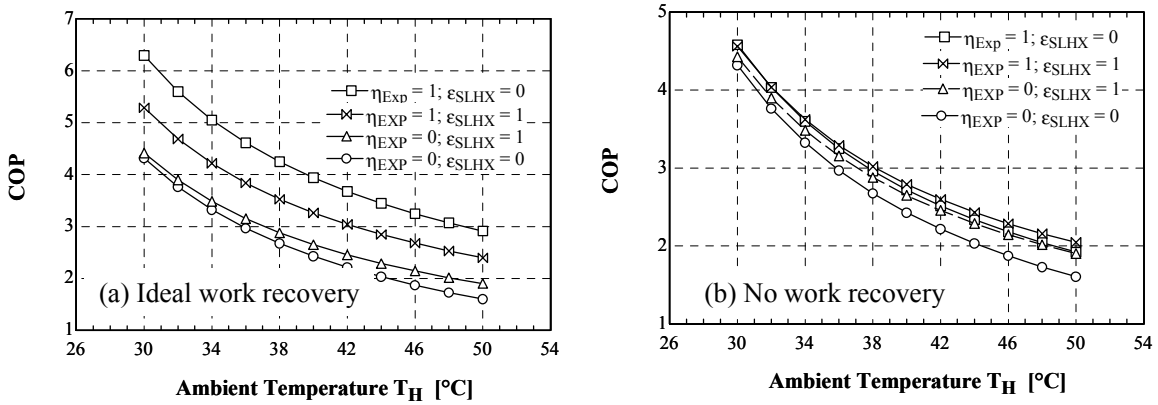

Figure 3: Performance of CO_2 system with expander and SLHX

An SLHX does not improve the COP of an expander system with ideal work recovery (Figure 3 (a)). If the expander work is not recovered, the system performance benefits from an SLHX at higher ambient temperatures. At an ambient temperature of 50°C, the benefit of an additional SLHX is in the order of 5% compared to the COP of a cycle without an SLHX. At lower ambient temperatures, an additional SLHX has no effect on the COP. As the degree of work recovery increases, the benefit of an SLHX installed in addition to the expander decreases. If more than 30% of the expander work can be recovered, the SLHX does not improve the system performance in the temperature range considered in Figure 3. In order to investigate the optimum cycle configuration depending on the degree of work recovery, the cycle performance has been optimized numerically with the independent variables expander efficiency, SLHX effectiveness and high-side pressure. The ambient temperature was constant at 50°C and the degree of work recovery ($\eta_{Recovery}$) was varied from 0% to 100% in 10% increments. The results indicate an abrupt transition from an optimum configuration with SLHX to the optimum configuration without the heat exchanger (Table 2). This means that no "optimum SLHX

effectiveness" other than a perfect SLHX (at low degrees of work recovery) or no heat exchanger at all (at high degrees of work recovery) exists.

Table 2: Optimum expander efficiency and SLHX effectiveness vs. work recovery

$\eta_{Recovery}$ [%]	η_{Exp} [%]	ε_{SLHX} [%]	P_{high} [kPa]	COP
0	100	100	12371	2.05
10	100	100	12336	2.08
20	100	100	12298	2.11
30	100	0	13275	2.13
40	100	0	13163	2.21
50	100	0	13035	2.30
60	100	0	12895	2.4
70	100	0	12741	2.50
80	100	0	12568	2.62
90	100	0	12371	2.76
100	100	0	12142	2.91

As the expander efficiency of a realistic system deviates from 100%, the degree of work recovery from which an SLHX improves the cycle performance will shift towards higher values. Conversely, as the pressure drop in a realistic SLHX increases, the degree of work recovery from which the SLHX reduces the cycle performance will shift towards lower values.

In order to understand the effect of an SLHX on the system performance, it is helpful to compare the cycles in a P-h diagram (Figure 4). The indices *C* and *E* indicate compressor and expander, respectively. The indices *1* and *2* indicate the cycle without and with SLHX, respectively.

Table 3 lists the specific work terms and cooling capacities presented in Figure 4.

Table 3: Specific work and cooling capacity for CO_2 cycle

	Without SLHX with expander	With SLHX with expander	Without SLHX, without expander
q [kJ/kg]	116.6	163	117.4
w_C [kJ/kg]	39.4	54	42.5
w_E [kJ/kg]	11.9	7.5	0
mfr [kg/s]	0.04288	0.03062	0.0426
COP	4.24	3.51	2.76

The values indicate that the increase in specific cooling capacity is compensated by the decrease in expander work and the increase in compressor work. The SLHX shifts the expansion process towards the left in the P-h diagram and the compression process towards the right. Since the slope of the lines of constant entropy in the diagram increases from right to left, this results in an increase in compressor work and a decrease in expander work.

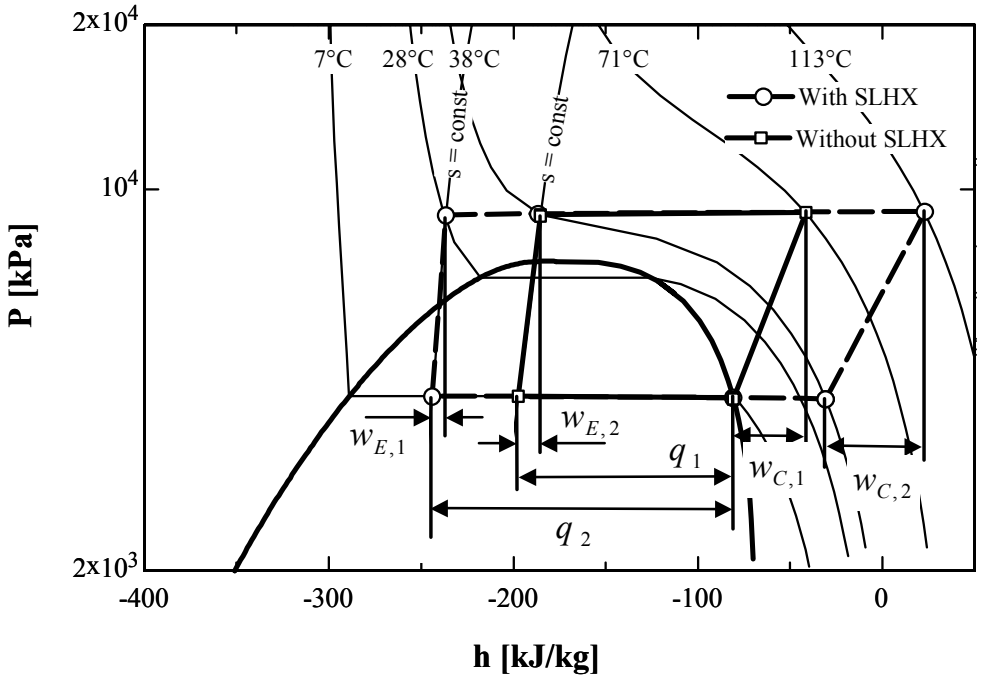

Figure 4: Expander work with and without SLHX

5 EXPANDER AND COMPRESSOR SIMULATION

In order to estimate the performance of realistic compressors and expanders, a general simulation of positive displacement machines has been developed. The algorithm calculates the performance of the devices accounting for valve losses, internal leakage, internal heat transfer, and unmatched volume ratio. Inputs to the program are the boundary conditions within which the compression/expansion takes place and geometric data of the positive displacement device. Outputs of the simulation are the thermodynamic state during the process, mass flow rate, work, and heat transfer to/from the fluid, and the gas forces and moments acting on the moving surfaces and the drive shaft. The algorithm is implemented in Matlab Release 12 and uses CEEEProps, an interface to Refprop 7, to calculate fluid properties. The program provides a graphical user interface for the simulation of single operating points and an interface to Microsoft Excel for batch operation.

5.1 Assumptions

Fluid Properties

The fluid properties in a control volume are average (bulk) properties. It is assumed that the properties are constant during each time step. The properties are calculated for thermodynamic equilibrium. Hence, the process is simulated as a quasi-steady-state process.

Valves

All valves are modeled as ideal valves. Pressure actuated (reed) valves are assumed to open fully and without any time delay. Position actuated valves, e.g. in scroll expanders, are assumed to open and close fully and instantaneously. Flow through the valves is simulated as flow through circular orifices.

All valves in expanders are simulated as position actuated valves. In expanders, it is not possible to use reed valves. For a valve to respond according to pocket and reservoir pressures, an external control is necessary. However, it is challenging to build an externally controlled valve that acts fast enough and has an acceptable flow resistance for typical residential AC applications (Maurer and Zinn 2000, Heyl 2000, Preissner 2001, Baek et al. 2002). With the timing of suction and discharge tied to the crankshaft angle, all expanders have built-in volume ratios. If the built-in (ideal) volume ratio does not match the volume ratio imposed on the expander by the boundary conditions (real volume ratio), the indicated efficiency decreases due to over- or under-expansion. The effect of over- and under-expansion is explained in Figure 5

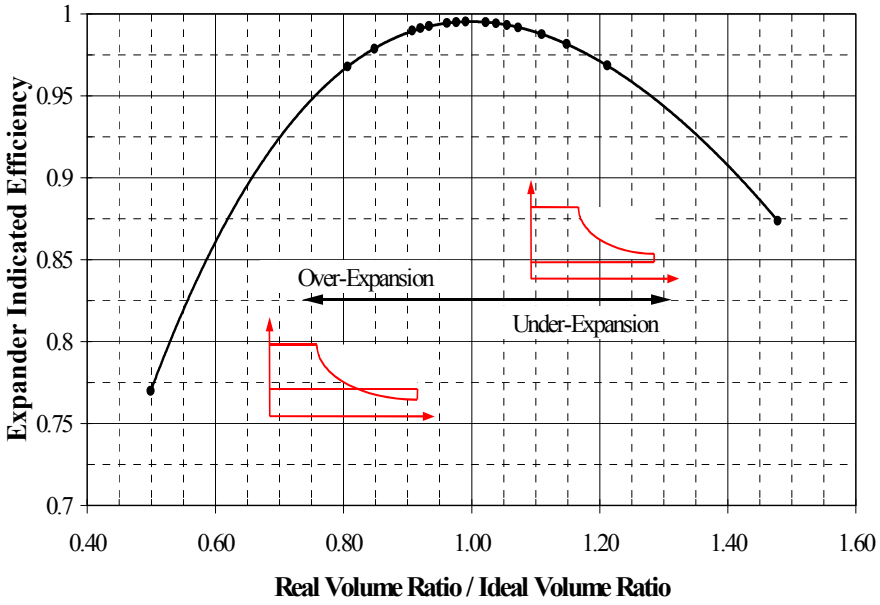

Figure 5 : Effect of over- and under-expansion on indicated efficiency of expander

Oil

The presence of oil in the control volume is neglected, unless oil contributes significantly to refrigerant leakage (see *Leak Flow* in Section 5.2.2). For the analysis of compressor and expander mechanisms in the report, only the rotary piston compressor was modeled with the effect of oil.

5.2 Modeling Approach

The algorithm is based on a discretization of the process into a number of time steps, following a control volume through the transient process from inlet to compression/expansion to discharge. At each time step, the irreversible processes of mass and heat flow are estimated. For each time step, a number of parallel control volumes can exist simultaneously. In a scroll compressor, for instance, two parallel control volumes are formed at the end of the suction process. These two control volumes are then compressed and finally merge into a single control volume at the center of the scroll.

The simulation of an expander starts at the intake process. At the beginning of the intake process, the crankshaft is at rotation angle zero. As the shaft turns, gas is flowing into the pocket and the crankshaft angle increases. At a specific angle, the pocket seals from the intake reservoir, and the gas is expanded. When the shaft reaches the discharge angle, the pocket opens to the low-pressure reservoir and the gas is expelled from the chamber. The crankshaft angle at which one cycle is completed depends on the type of expander. For a reciprocating piston expander, for instance, the process ends at crankshaft angle 2π. For a rotary piston, the process ends at an angle of 4π. For a scroll expander, the angle depends on the length of the wraps.

The process in a compressor is modeled as a reverse expansion process. The simulation starts with the suction process at the highest value of the crankshaft angle. As the suction pocket seals from the low-pressure reservoir and the gas is compressed and finally discharged, the value of the crankshaft angle decreases until it reaches zero when the cycle is completed.

5.2.1 Geometric Data

Geometric information about the device is required at each time step. These data are:

- Rotation angle of the crankshaft
- Control volume
- Projection of moving surfaces into x-, y-, and z-direction
- Position of moving surfaces with respect to coordinate system
- Leak paths: The data for the leak path contain topological information about the device, indicating the pockets adjacent to the control volume being followed
- Dimensions of each leak path

Additional information required:

- Device type
- Conversion factor of dimensions used to SI units
- Number of parallel control volumes
- Crankshaft angle at which discharge and suction port uncover
- Number of leak paths
- Type of each leak path

The geometric information is provided in an ASCII text file. For an expander, the tables are read from position 1 to end, for a compressor, the tables are read in reverse order. An example for a scroll device is offered in Appendix B.

5.2.2 Thermodynamic Simulation

Each time step is considered a sequence of two separate processes:

(1) Isentropic change of volume at constant mass (process $1 - 2^*$)

$$s_2^* = s_1 \qquad \text{Equation 3}$$

$$m_2^* = m_1 \qquad \text{Equation 4}$$

$$\rho_2^* = m_2^* / V_2 \qquad \text{Equation 5}$$

$$u_2^* = u\left(s_2^*, \rho_2^*\right) \qquad \text{Equation 6}$$

(2) Change of mass and internal energy due to mass and heat transfer at constant volume (process 2^* - 2)

$$m_2 = m_2^* + \sum m_{Valve} + \sum m_{Leak} \quad \text{Equation 7}$$

$$U_2 = u_2^* \cdot m_2^* + \sum H_{Valve} + \sum H_{Leak} + \sum Q \quad \text{Equation 8}$$

$$u_2 = U_2 / m_2 \quad \text{Equation 9}$$

$$\rho_2 = m_2 / V_2 \quad \text{Equation 10}$$

$$s_2 = s(u_2, \rho_2) \quad \text{Equation 11}$$

Valve Flow

The instantaneous mass flow rates through the valves are simulated as incompressible flow through an orifice.

(a) Single phase (White 1994)

$$\dot{m}_{Valve}(t) = C_d \cdot A_{Valve} \cdot \sqrt{\frac{2\rho_{up}\Delta P}{1-\beta^4}} \quad \text{Equation 12}$$

$$C_d(t) = 0.5959 + 0.0312\beta^{2.1} - 0.184\beta^8 + \left(0.0029\beta^{2.5}\right)\left(10^6 / Re(t)\right) \quad \text{Equation 13}$$

$$\beta = 0.3 \quad \text{Equation 14}$$

(b) Two phase flow (Lin 1982)

$$\dot{m}_{Valve}(t) = C_d(t) \cdot A_{Valve}(t) \cdot \sqrt{\frac{2\rho_{up}(t)\Delta P(t)}{\left(1-\beta^4\right) \div \left[\left(1-x_{up}\right)\Theta(t) + x_{up}\sqrt{\rho_L(t)/\rho_G(t)}\right]}} \quad \text{Equation 15}$$

$$\Theta(t) = 1.48625 - 9.26541 r_d(t) + 44.6954[r_d(t)]^2 - 60.615[r_d(t)]^3 - 5.12966[r_d(t)]^4 - 26.5743[r_d(t)]^5 \quad \text{Equation 16}$$

C_d and β as for single phase flow

The enthalpy flow rate through a valve is obtained by multiplying the mass flow rate with the upstream specific enthalpy. The valve flow is checked for choked flow by comparing the computed flow velocity against the speed of sound at the upstream conditions.

The effective flow area A_{Valve} is simply the cross sectional area of the port. Valve motion is not considered, clearly overestimating the valve performance. This simplification was made in order to obtain best-case results. Additional losses due to non-ideal valve motion can be simulated using smaller port diameters.

Heat Flow

The heat transfer in compressors has been studied by a number of researchers with contradicting results (Brok et al, 1980). Most research has focused on heat transfer in reciprocating piston compressors. Typically, the instantaneous heat flow rate is described by Newton's approach

$$\dot{Q}(t) = h(t) \cdot A_Q(t) \cdot [T_{Wall} - T(t)]. \qquad \text{Equation 17}$$

The heat transfer coefficient *h(t)* is obtained from a function of the type

$$Nu(t) = a \cdot [\mathrm{Re}(t)]^b \cdot \mathrm{Pr}^c . \qquad \text{Equation 18}$$

Various values for the coefficients and for the definition of the Reynolds number have been proposed. The effect of heat transfer on the performance of CO_2 compressors and expanders is discussed in Section 6.3.

The temperature T_{Wall} is the effective wall temperature of the control volume. In a realistic device, the wall temperature varies with location and time. In the simulation however, an average time-independent wall temperature is assumed. The effect of heat transfer on the performance of compressors and expanders in residential air-conditioning applications is discussed in Section 6.3

Leak Flow

Although internal leakage has a significant effect on the performance of positive displacement compressors, little research has been undertaken to derive correlations for the instantaneous leakage mass flow rates that are dependent on geometry and driving pressure difference. In the open literature, isentropic compressible flow, adiabatic viscous compressible flow, and incompressible flow models are proposed (Fukuta et al. (2002). Most of the experimental research has been carried out on the leakage flow of air at room temperature and pressures below 1 MPa. Other researchers investigated leakage using conventional refrigerants (Ishii 1996).

The instantaneous leak flow rates are computed assuming incompressible viscous flow and accounting for frictional losses and minor losses due to entrance and exit effects. The computed flow velocity is checked against the speed of sound and corrected for choked flow. In order to achieve a smooth transition from laminar to turbulent flow the leak flow rate is computed as

$$\dot{m}_{Leak}(t) = \sqrt[20]{\left[\dot{m}_{Leak}^{Laminar}(t)\right]^{20} + \left[\dot{m}_{Leak}^{Turbulent}(t)\right]^{20}}, \qquad \text{Equation 19}$$

where

$$\dot{m}_{Leak}^{Laminar}(t) = \frac{-4\mu w L}{k_m \delta} + \sqrt{\left(\frac{-4\mu w L}{k_m \delta}\right)^2 + \frac{\rho (w\delta)^2}{k_m} \Delta P} \quad \text{and} \qquad \text{Equation 20}$$

$$\dot{m}_{Leak}^{Turbulent}(t) = \sqrt{\frac{\rho(w\delta)^2}{0.01875 \cdot L/\delta + k_m}\Delta P}\,. \qquad \text{Equation 21}$$

The effective diameter is 2/3 of the hydraulic diameter (White 1994), the friction factor for turbulent flow is 0.075 (fully rough flow channel), and the coefficient for minor losses is 1.5, assuming a coefficient of 0.5 for the entrance losses and 1 for the exit losses.

There are two different types of leak paths in the compressors and expanders investigated: the tip leak and the flank leak. The tip leak is a flow passage of small height and large width. This type of leak is found, for example, in a scroll device between the top of the wall and the base plate of the other scroll or in a piston device between the piston and the cylinder wall. The flank leak is a flow passage between two curved walls and is found in a scroll device between two adjacent wraps or in a rotary piston machine between the roller and the cylinder wall. Preissner (2001) showed that the length of the flank leak path can be expressed as the curvature difference *cd*

$$cd = 1/r - 1/R\,, \qquad \text{Equation 22}$$

where r and *R* are the radii of the channel wall with the greater and smaller curvature, respectively.

In some compressors (e.g. rotary piston), oil is used to improve sealing. In this case, refrigerant may leak from a high-pressure control volume to a low-pressure control volume via a so-called oil-leak. Refrigerant from the high-pressure pocket dissolves in oil and evaporates from the oil as the mixture enters the low-pressure pocket. In this case, the leakage mass flow rate of CO_2 is estimated to be 10% of the oil mass flow rate. The mass flow rate of oil is computed using Equation 19 through Equation 22 using a constant viscosity of 20 mPas (Hauk, Weidner, 2000), assuming a saturated PAG oil-CO_2 mixture at 100°C and 10 MPa.

5.2.3 Solution Scheme

The simulation of the compression/expansion process consists of two problems:

(1) Numerical integration transient process from suction to discharge
(2) Numerical solution of the leakage flow rates to satisfy conservation of mass and energy

The numerical integration solves the problem

$$f(t) = f_0 + \int y(f,t)dt\,, \qquad \text{Equation 23}$$

where *f(t)* is the mass or energy contained in the control volume, f_0 is an initial condition, *y(f, t)* is the mass or energy flow rate, and *t* is time. For the valve and heat flow rates, a fourth order Runge-Kutta method is used.

Using a step-by-step method, such as Runge-Kutta, for the leak flow rates may result in violation of conservation of mass or energy. The difference between the valve and heat flow and the leak flow is that the valve and heat flow only affects the control volume in question, while the leak flow also affects control volumes of previous or future time steps. This is especially apparent in devices with several pockets interacting with each other, for example in a scroll compressor. Shortly after a control volume has been formed in the suction process, it may be connected via a leak with a pocket closer to the center of the scroll and some amount of mass may leak to into the control volume, resulting in a pressure increase. After one rotation of the crankshaft, the control volume may be exactly at the point where the high-pressure pocket was. The control volume communicates now with a pocket closer to the perimeter of the scroll, which has a higher pressure than at the previous instance. Thus, the pressure difference and hence the mass flow rate is smaller. Consequently, the control volume and the low-pressure pocket contain more mass than there was before, resulting in a violation of the conservation of mass and energy, as well as in the destruction of entropy.

In order to avoid this type of problem, the leak flow rates are computed simultaneously for all time steps. Starting with an initial guess for the leak flow rates at all time steps (for instance, all flow rates are zero), the integration is carried out, producing a mass and internal energy profile in the device for the time interval from suction to discharge. Based on this pressure profile, the leak flow rates are computed. In order for the solution to represent the compressor/expander at steady operation, the pressure and enthalpy field must not change when the newly computed leak flow rates are reapplied. Conversely, the leak flow rates of two subsequent iterations must be equal. This means the leak flow rates must produce the same pressure and enthalpy field from which they were computed

$$\dot{m}_{Leak} = F\left(\dot{m}_{Leak}\right) \text{ and}$$
$$\dot{H}_{Leak} = F\left(\dot{H}_{Leak}\right), \qquad \text{Equation 24}$$

where F is a system of equations consisting of Equation 19 through Equation 21 with the mass and energy field in the compressor/expander as variables. Mathematically, this can be interpreted as the flow rates being the eigenvector to the linear map F. This means that the solution flow rates are fixed points to the system of equations F. Following these observations, Equation 24 is solved using a fixed-point iteration scheme

$$\dot{m}_{j+1}^{Leak} = F\left(\dot{m}_{j}^{Leak}\right)$$
$$\dot{H}_{j+1}^{Leak} = F\left(\dot{H}_{j}^{Leak}\right) \qquad \text{Equation 25}$$

Convergence is reached when

$$\left|\dot{m}_{j}^{Leak} - \dot{m}_{j-1}^{Leak}\right| < \varepsilon \text{, or}$$
$$\left|\overline{P}_{j} - \overline{P}_{j-1}\right| < \varepsilon \qquad \text{Equation 26}$$

where $\overline{P}$ indicates the pressure field.

5.2.4 Step Size Adaptation

The error in the numerical integration depends strongly on the size of the time intervals. In order to reduce the error while keeping the computational time within limits, the step size is refined only where the error is large. The step size is reduced if the dependency of mass and internal energy on mass flow and heat transfer is strong

$$\left|\partial f_j / \partial y_j\right| \Delta t_n > \varepsilon , \qquad \text{Equation 27}$$

where the criterion ε can be determined by the user.

5.2.5 Boundary Conditions

The performance of a compressor or expander depends on the boundary conditions within which it operates. For the simulation developed in this project, the following boundary conditions are considered:

- Angular speed
- Pressure and density of the fresh suction gas, entering the suction reservoir from the evaporator (compressor simulation) or gas cooler (expander simulation)
- Pressure in the discharge reservoir
- Control volume wall temperature

Further parameters affecting the performance are:

- Leakage gap size (machining tolerances)
- Inlet and outlet port area

6 SIMULATION RESULTS

Section 6.1 defines the performance characteristics of compressors and expanders used in this report. With the boundary conditions (inlet pressure, inlet density, wall temperature) and the machining tolerance (leakage gap size) as independent variables, the compressor and expander performance is a function of four variables. If any of the variables can be neglected in the generation of performance maps, the computational time can be reduced significantly. In Sections 6.2 and 6.3, the superheat at the compressor inlet and the internal heat transfer in compressor and expander are demonstrated to produce an insignificant effect on the performance. Hence, the compressor inlet density and the wall temperature for compressor and expander can be neglected. In Section 6.4, the geometric design of possible candidates for compressors and expanders in residential CO_2 air-conditioning systems is optimized. Section 6.5 discusses the results of the optimization.

By convention, an expansion process is modeled with increasing crankshaft angle from intake to discharge. A compression process is modeled with decreasing shaft angle from suction to discharge (see Section 5.2). All angles are given in radians.

6.1 Performance Characteristics

The indicated and volumetric efficiencies are used to characterize the performance of the analyzed compressors. The expanders are characterized by the indicated efficiency and the volumetric flow rate coefficient. Knowing the displacement volume and the boundary conditions (inlet state, discharge pressure, and possibly wall temperature), these parameters can be translated into the mass flow rate delivered and the work input or output. The indicated efficiency is defined as

$$\eta_{ind} = \begin{cases} \dfrac{W_{is}}{W_{real}} = \dfrac{h(s_{in}, P_{out}) - h(s_{in}, P_{in})}{h(s_{out}, P_{out}) - h(s_{in}, P_{in})} & \textit{Compressor} \\ \dfrac{W_{real}}{W_{is}} = \dfrac{h(s_{out}, P_{out}) - h(s_{in}, P_{in})}{h(s_{in}, P_{out}) - h(s_{in}, P_{in})} & \textit{Expander} \end{cases} \qquad \text{Equation 28}$$

The volumetric efficiency η_{vol} and the volumetric flow rate coefficient ε_{vol} are defined as

$$\eta_{vol} = \frac{\dot{m}_{real}}{\rho_{in} \cdot V_{displ}} \quad \textit{Compressor}$$

$$\varepsilon_{vol} = \frac{\dot{m}_{real}}{\rho_{in} \cdot V_{\max}} \quad \textit{Expander} \qquad \text{Equation 29}$$

where V_{displ} is the compressor displacement volume and V_{max} is the maximum volume during the course of a control volume from inlet to outlet (e.g. the geometric cylinder volume in a piston expander or the volume of the two most outer pockets in a scroll expander). An ideal expander has a volumetric flow rate coefficient equal to the inverse

of its optimum volume ratio. This characterization parameter for the expander is chosen because it bases the inlet volume purely on the geometry of the device and eliminates any effect of the operating conditions on the definition of the suction volume. The volumetric flow rate coefficient can be understood as a dimensionless volume flow rate through the expander per revolution. In an expander, the direction of the flow though the expander is in the same direction as the pressure gradient, preventing the definition of a volumetric efficiency with the same significance as that of a compressor.

6.2 Effect of Inlet Density on CO_2 Compressor Performance

The effect of inlet density is studied on the example of a reciprocating piston compressor. The piston mechanism has losses due to internal leakage and valve losses. Internal heat transfer is not considered in this analysis. It is assumed that the results for the reciprocating piston can be transferred to other mechanisms.

Figure 6 shows the indicated and volumetric efficiency of a piston compressor over a range of values for the suction density at constant suction and discharge pressures. The range of the inlet density represents a degree of suction superheat from 0 K to 20 K. The indicated and volumetric efficiencies change by less than 2% over the range of super heat considered. Therefore, the effect of super heat on the compressor performance is neglected in the simulation.

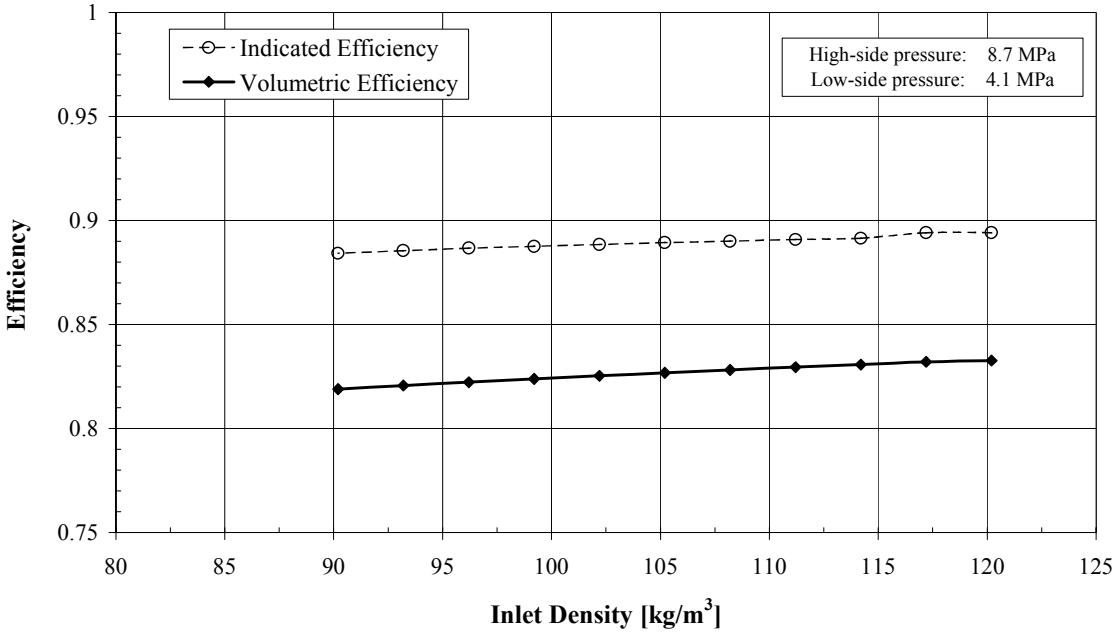

Figure 6: Effect of inlet density on compressor performance

The effect of inlet density on the performance of an expander cannot be neglected since it affects the volume ratio and hence the indicated efficiency.

6.3 Effect of Heat Transfer on CO_2 Compressor and Expander Performance

Heat transfer between the fluid contained in a control volume and the wall of the control volume depends on the surface area of the wall, wall and fluid temperatures, and the heat transfer coefficient between wall and fluid. The surface area is given by the geometry of the device. The wall temperature is given as a boundary condition, and the fluid temperature is solved for. The heat transfer coefficient depends on the fluid state and the fluid movement in the control volume. The fluid movement varies with time and depends strongly on the geometry of the control volume.

Compressor

Adair et al. (1972) proposed a correlation for the instantaneous heat transfer in a piston compressor, which is intended to reflect the effect of the transient velocity field in the pocket and yet does not require detailed flow simulations. In the correlation the Reynolds number *Re* is based on the swirl velocity $\omega_g(t)$ in the pocket, which itself is a function of compressor angular velocity ω and the crankshaft angle $\varphi(t)$:

$$\omega_g(t) = \begin{cases} 2\omega[1.04 + \cos(2\varphi)] & \pi/2 < \varphi < 3\pi/2 \\ \omega[1.04 + \cos(2\varphi)] & \varphi < \pi/2 \text{ or } \varphi > 3\pi/2 \end{cases} \quad \text{Equation 30}$$

$$Re(t) = \frac{\rho(t)[D_e(t)]^2 \omega_g(t)}{2\mu(t)} \quad \text{Equation 31}$$

$$D_e(t) = \frac{6 \cdot Volume(t)}{Area} = \frac{3/2\, D \cdot S(t)}{S(t) + D/2} \quad \text{Equation 32}$$

with *S(t)* the stroke length, *D* the piston diameter, and ρ the fluid density. The heat transfer coefficient is then obtained from the Nusselt number given by

$$Nu(t) = 0.053[Re(t)]^{0.8}[Pr(t)]^{06} \quad \text{Equation 33}$$

$$Nu(t) = \frac{h(t)D_e(t)}{k(t)} \quad \text{Equation 34}$$

The correlation was used to study the effect of heat transfer on the performance of CO_2 piston compressor. Figure 7 is a plot of the Nusselt number for CO_2 at different angular velocities. The plot shows one complete piston stroke from top dead center at 2π over bottom dead center at π and back to top dead center at *0*. The points of discontinuity at angles of $\pi/2$ and $3\pi/2$ are due to the discontinuous function for the swirl velocity (see Equation 30). The swirl velocity undergoes a sudden change when the piston movement changes from acceleration to deceleration.

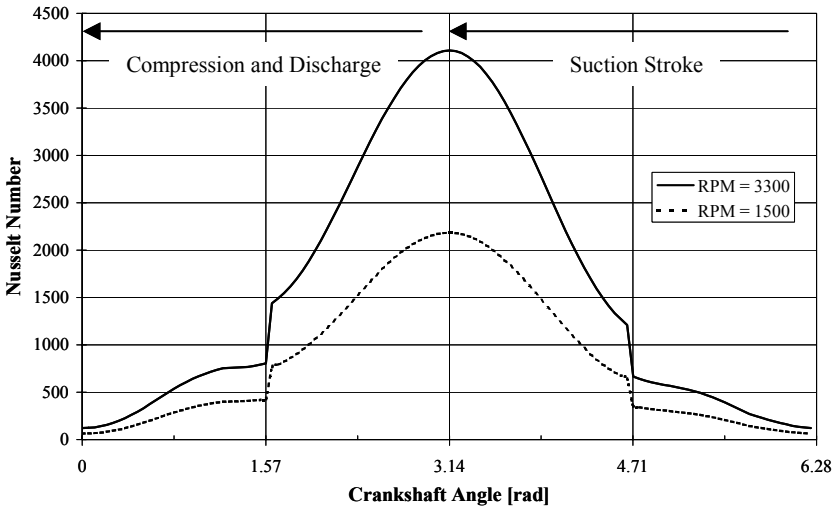

Figure 7 : Instantaneous heat transfer coefficient in piston compressor

Figure 8 and Figure 9 show the isentropic and volumetric efficiency ratios versus the pocket wall temperature for different values of the angular speed. The efficiency ratio is the ratio of the efficiency with heat transfer compared to the appropriate efficiency without heat transfer. The adiabatic operating points designate the wall temperatures at which the sum heat transfer into and out of the fluid is zero (~23°C for all angular speeds). The graphs show that the change in efficiency is less than 1% in the significant range of operating conditions.

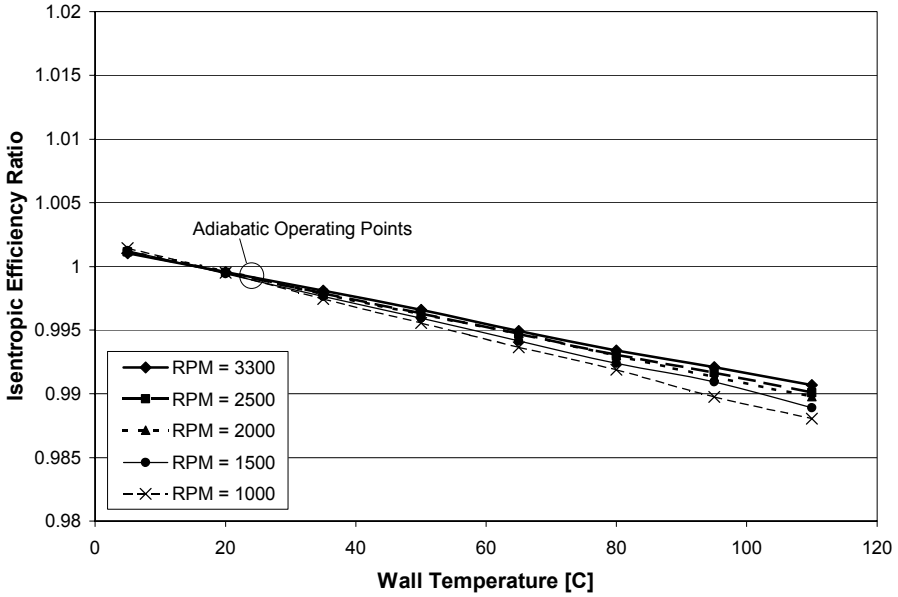

Figure 8: Isentropic efficiency versus piston compressor wall temperature

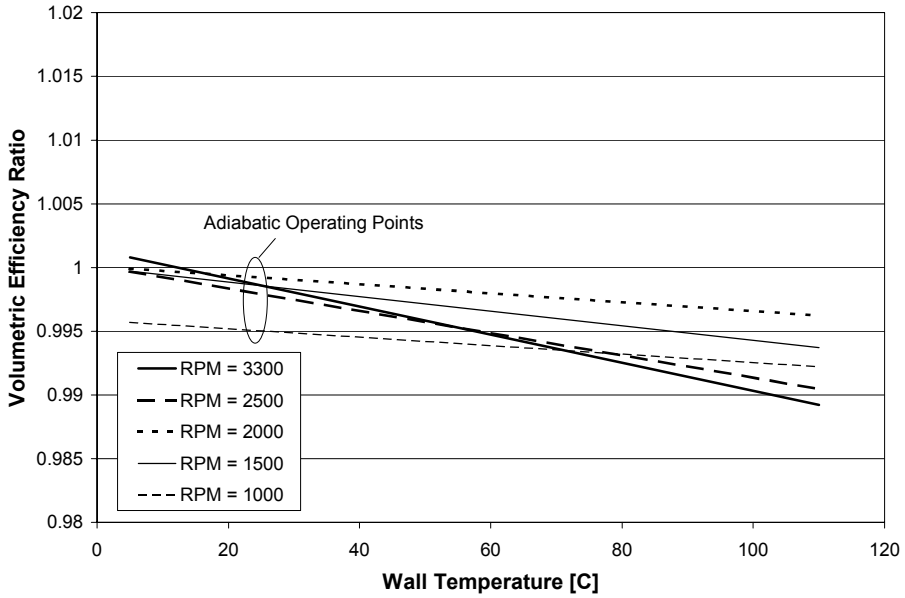

Figure 9: Volumetric efficiency versus piston compressor wall temperature

The small effect of internal heat transfer is due to the short time interval that the gas is in contact with the compressor wall and to the reversal of the direction of the heat transfer during the compression.

In order to support the assumption that internal heat transfer in a compressor for the current application is insignificant, the effect of heat transfer in a scroll compressor is investigated. Research on the gas to wall heat transfer in scroll compressors could not be found in the open literature. Therefore, an approach for turbulent pipe flow is used. The heat transfer coefficient is given by a Nusselt number relationship

$$Nu_{turb} = 0.023 \cdot Re^{4/5} \cdot Pr^{2/5} \qquad \text{Equation 35}$$

where the Reynolds number is based on the rate of volume change in the device

$$Re = \frac{\left|\left(V_{prev}/V\right)^{1/3} - 1\right|}{\Delta t} \cdot \left(\frac{3V}{4\pi}\right)^{2/3} \cdot \frac{\rho}{\mu}. \qquad \text{Equation 36}$$

Figure 10 shows the instantaneous Nusselt number in a scroll compressor. The plot follows a compression chamber from the position where the pocket is just sealed from the suction reservoir at approximately *10.5* rad to complete discharge with pocket volume equal to zero at crankshaft angle *0*. With increasing pocket pressure and density, the Nusselt number increases. As the two pockets merge at 2π, the pocket volume increases suddenly, resulting in an increase of the Nusselt number. During most of the discharge process (2π to *0*), the Nusselt number is approximately constant, reflecting the constant fluid properties during this process. At the end of the discharge process, the rate of change of the pocket volume decreases, resulting in a decreasing Nusselt number.

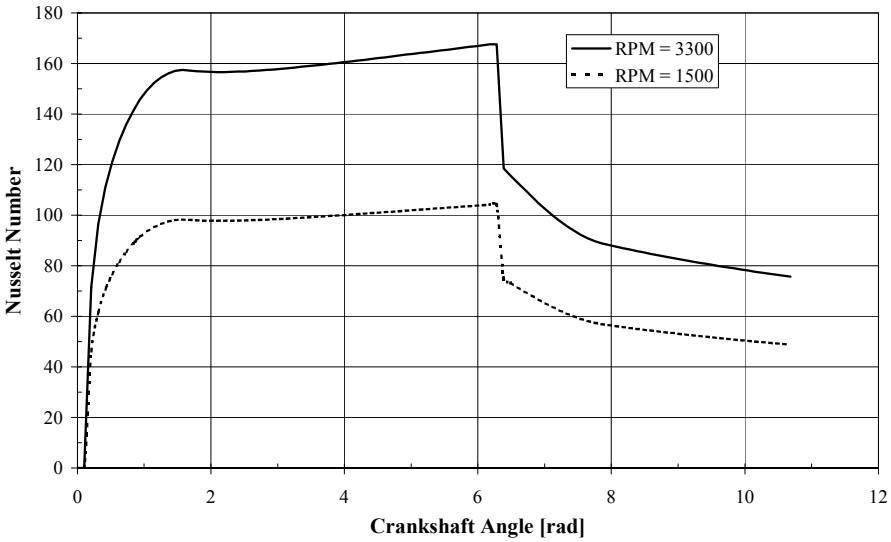

Figure 10 : Instantaneous heat transfer coefficient in scroll compressor

Figure 11 is a plot of the instantaneous heat flow rate in the scroll compressor over a range of wall temperatures between 5°C and 100°C. The effect on the compressor performance is shown in Figure 12.

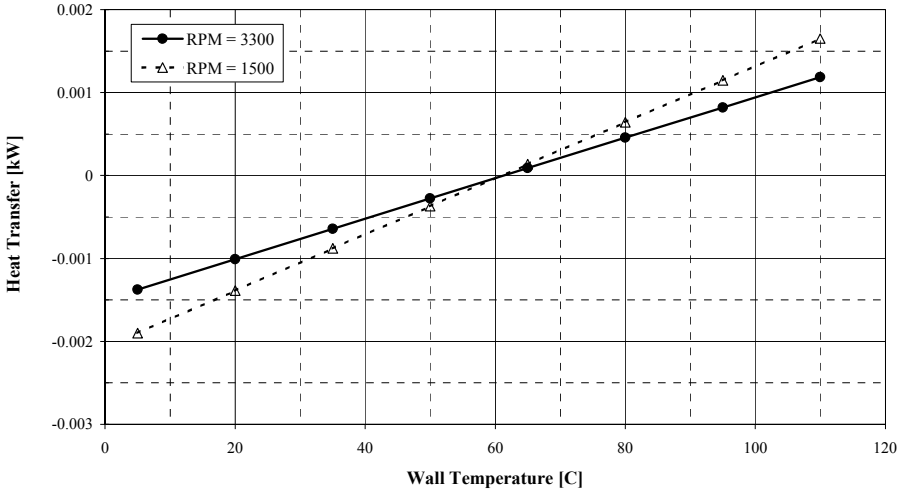

Figure 11: Instantaneous heat flow rate in scroll compressor

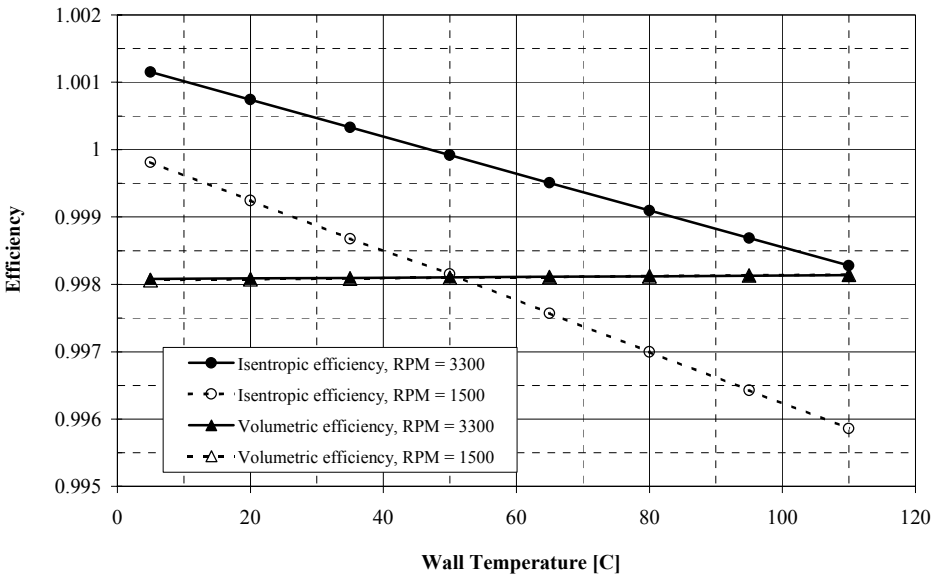

Figure 12: Volumetric and isentropic efficiency in scroll compressor with heat transfer

The plot shows that the compressor performance in affected by less than 1% over the range of wall temperatures considered. Hence, it seems safe to neglect internal heat transfer in the simulation of scroll compressors. These results support the conclusion that internal heat transfer in compressors can be neglected for residential CO_2 air-conditioning applications.

Expander

Little attention has been paid in the literature to internal heat transfer in positive displacement expanders. In the absence of experimental correlations for the heat transfer coefficient, modified correlations for the heat transfer coefficient in compressors are used. In addition to convection, the heat transfer in expanders is enhanced by evaporation of liquid refrigerant at the wall of the pocket. In turbulent pipe flow, the heat transfer coefficient is typically increased by a factor of five in the presence of evaporation. Therefore, the heat transfer coefficients obtained with Equation 33 are multiplied by five for expander simulations.

Figure 13 shows a plot of the instantaneous heat transfer coefficient in a piston expander, obtained using Equation 30 through Equation 34, versus the crankshaft angle. The expansion proceeds from angle *0* to 2π .

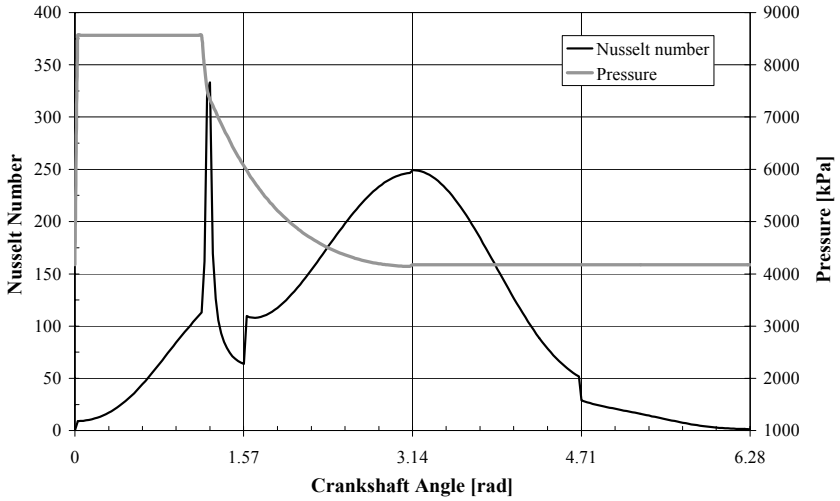

Figure 13: Instantaneous heat transfer coefficient in piston expander

The sudden increase of the heat transfer coefficient at crankshaft angle 1.25 is due to the change of fluid properties as the fluid enters the two-phase region. Figure 14 shows the heat transfer between fluid and wall for wall temperatures between 5°C and 110°C. The wall temperature at which the net heat transfer is equal to zero, approximately 30°C, represents the boundary condition for adiabatic operation.

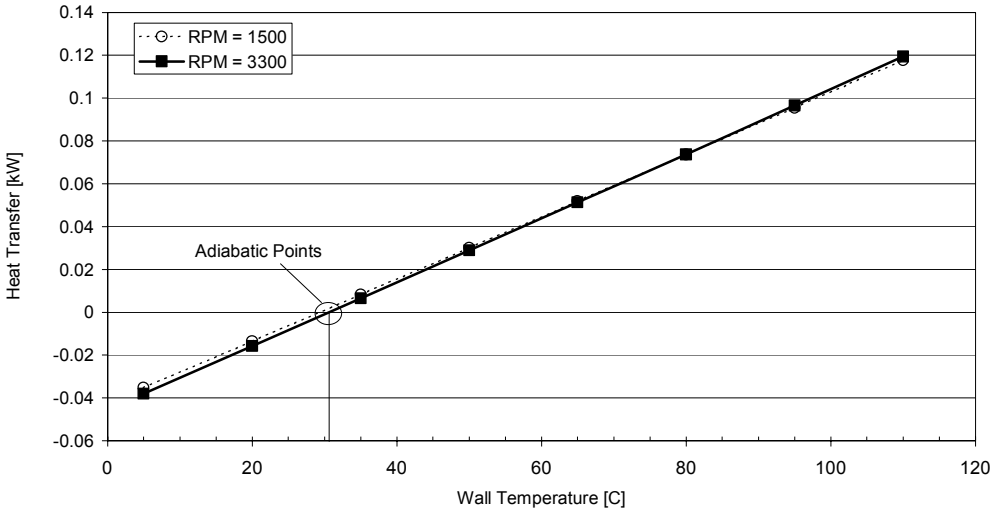

Figure 14: Net heat transfer between fluid and piston expander wall

The performance of the expander is shown in Figure 15. The volumetric and isentropic efficiencies are approximately constant for all wall temperatures considered (the isentropic efficiency changes with expander speed due to valve losses). This implies that the effect of internal heat transfer on the performance of a piston expander is negligible.

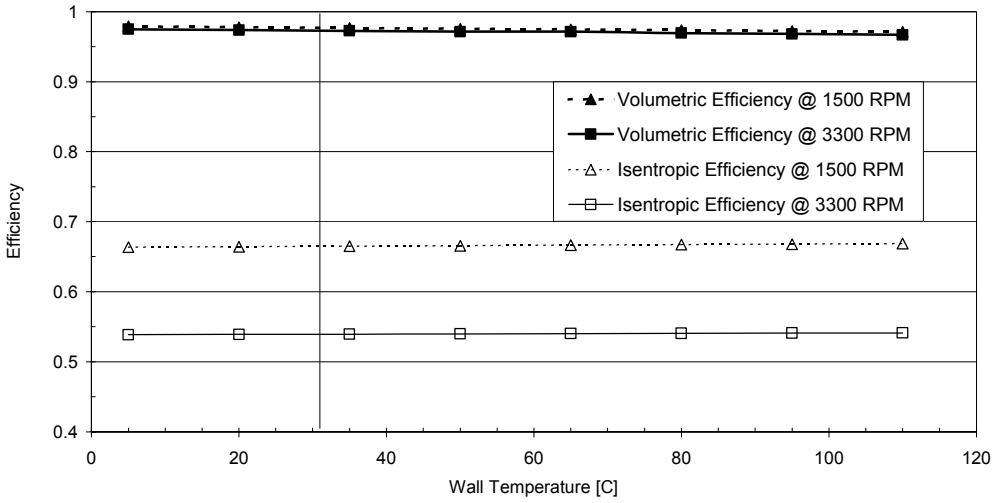

Figure 15: Piston expander performance versus wall temperature

Figure 16 shows the instantaneous Nusselt number in a scroll expander and the pressure in the expander pocket. At a crankshaft angle of approximately 6.3, the refrigerant enters the two-phase region and evaporation occurs, causing a sharp peak in the heat transfer coefficient due to changes in the fluid properties

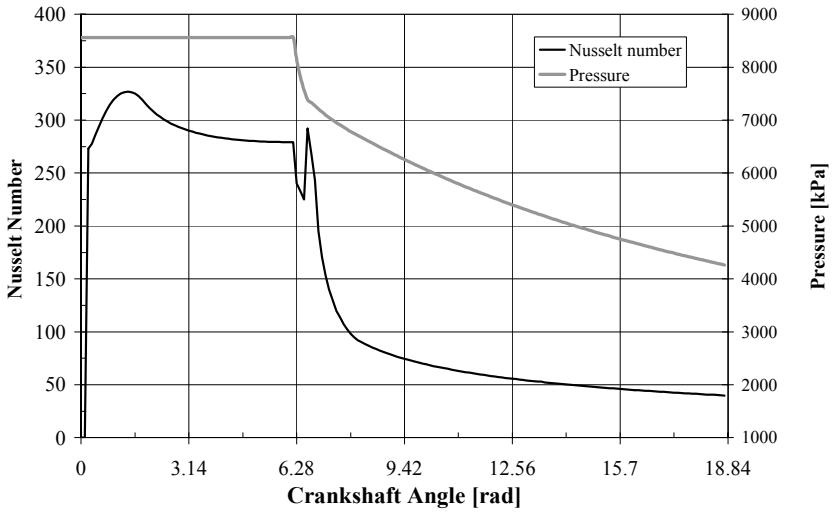

Figure 16: Instantaneous heat transfer coefficient in scroll expander

Figure 17 shows the instantaneous heat flow rates in the scroll expander. Comparing Figure 17 with Figure 11 shows that the flow rates in the expander have increased significantly. The adiabatic operating point of the expander is found where the net heat flow rate between the refrigerant and wall is zero. The device operates adiabatically at a wall temperature of approximately 25°C.

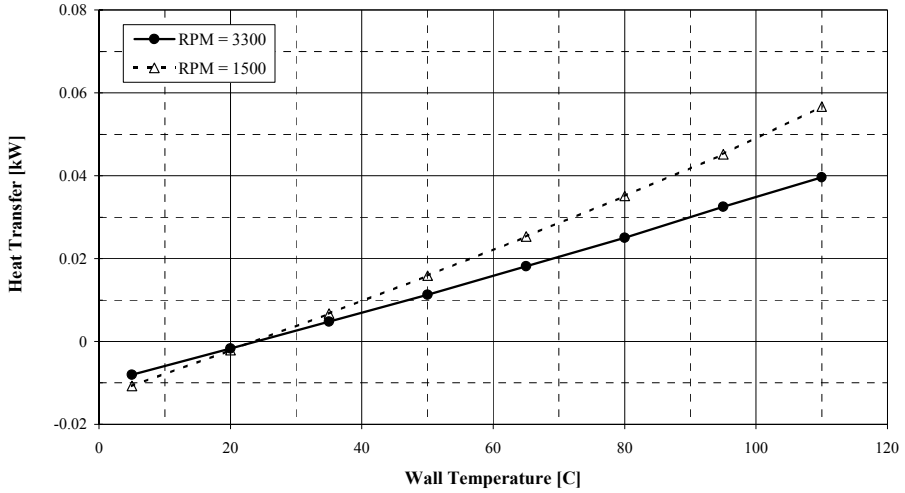

Figure 17: Instantaneous heat flow rate in scroll expander

Figure 18 shows the effect of heat transfer on the expander performance over a range of wall temperatures. The expander efficiency changes by up to 20%.

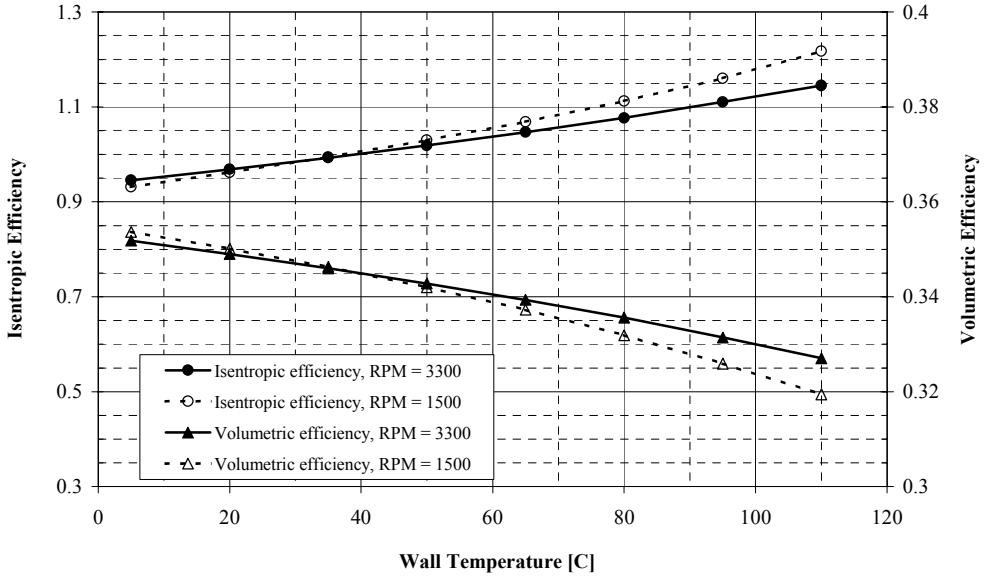

Figure 18: Volumetric and isentropic efficiency in scroll expander with heat transfer

Figure 19 compares the efficiency of the expander including heat transfer to the efficiency with no heat transfer between the wall and refrigerant. It is found that heat transfer affects the performance at adiabatic operating conditions (zero *net* heat transfer) by less than 3%.

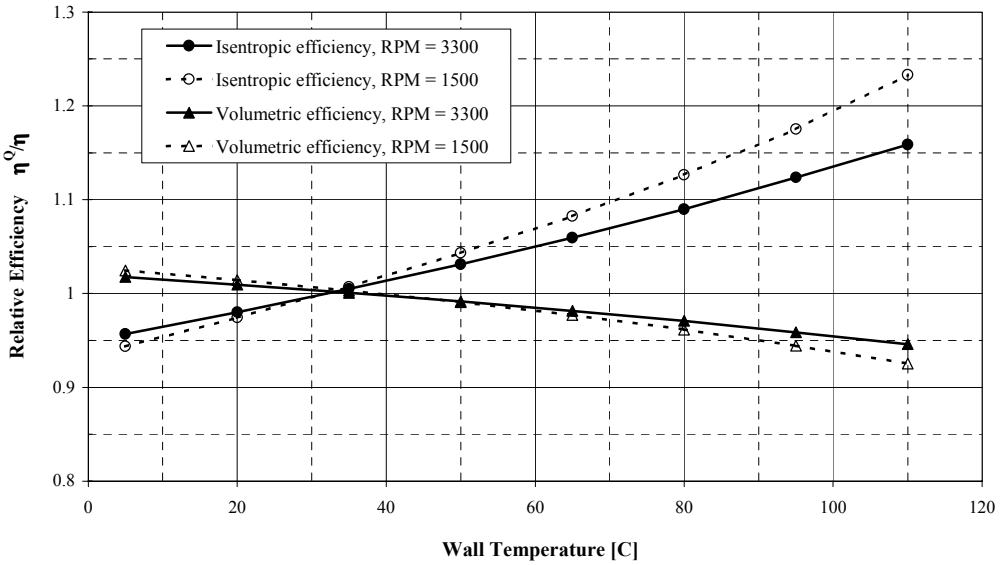

Figure 19: Scroll expander efficiency with and without heat transfer

If compressor and expander are combined in an integrated device, the two components are coupled through internal heat transfer. Assuming an insignificant heat resistance between compressor and expander, such that the temperature of the expander wall is equal to the wall temperature of the compressor, the integrated device operates adiabatically if the net heat transfer between expander and compressor is zero, according to

$$\left|\dot{Q}_{Compressor}\right| = -\left|\dot{Q}_{Expander}\right| \text{ and } T^{Wall}_{Compressor} = T^{Wall}_{Expander}.$$

Figure 20 shows the heat flow rates of the compressor and the negative flow rate in the expander. The adiabatic operating point of the integrated device is found where the two curves intersect. The process is dominated by the heat transfer of the expander due to the high heat transfer coefficient during evaporation. The adiabatic operating point of the integrated device is close to that of the expander alone. Therefore, the performance is not strongly affected by internal heat transfer (Figure 12 and Figure 19).

Considering the uncertainty in the correlation for the heat transfer coefficient and the small effect of heat transfer on the performance, it seems justified to neglect heat transfer in the simulation of scroll compressors and expanders.

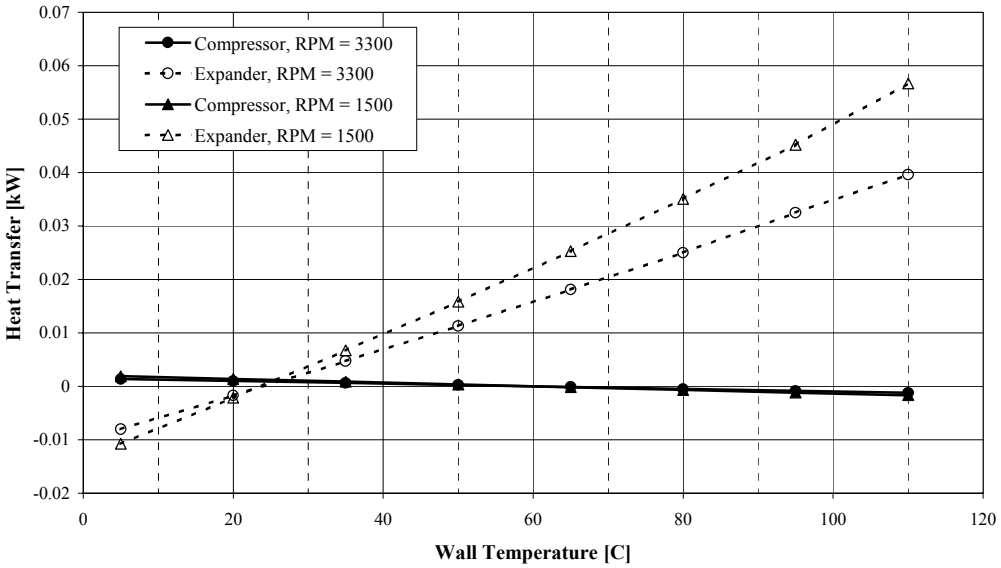

Figure 20: Heat flow rates in integrated scroll compressor-expander device

Thus far only heat transfer between the fluid and the pocket wall has been considered. However, a fluid also exchanges heat inside the compressor/expander before entering the compression/expansion compartment. This process is referred to as suction heating. The fluid in the suction reservoir is at suction pressure and close to suction temperature. The fluid heats up when it is in thermal contact with the reservoir wall. Suction heating reduces isentropic and volumetric efficiency. Since the direction of the heat transfer is never reversed in this process (as it is in internal heat transfer), the effect on performance is greater then the effect of internal heat transfer. The heat transfer coefficient for suction heating is obtained from a correlation for heat transfer in circular tube with turbulent flow. Caillat et al. (1988) and Lee and Kim (2001) used this method for the simulation of scroll compressors and found good agreement with experimental results.

6.4 Optimization of Compressor and Expander Geometry for Residential Air-Conditioning Applications

The performance of the following compressor and expander mechanisms has been analyzed[1]:

- Reciprocating piston
- Rotary piston
- Scroll

In order to make a fair comparison, the geometry of each individual mechanism has been optimized for use as compressor and expander under constant boundary conditions. The

[1] During the project meeting in January 2002, it was agreed to not consider the option of an expander based on the gear pump mechanism due to the limited indicated efficiency of the constant pressure expansion.

boundary conditions are given in Table 4. The values are chosen for a 10 kW CO_2 expander cycle at AHRAE A conditions with an assumed compressor and expander isentropic efficiency of approximately 75%. The approach temperature in the gas cooler is on the order of 3 K and the evaporating temperature is approximately 7°C. The cycle does not include an SLHX. The valve timing of the devices, which have a built-in volume ratio (all expanders and the scroll compressors), has been optimized for the individual operating conditions.

Table 4: Boundary conditions for compressor and expander optimization

	Compressor	Expander
P_{Inlet} [MPa]	4.126	8.563
ρ_{Inlet} [kg/m^3]	120.2	524.2
P_{outlet} [MPa]	8.676	4.174
Heat transfer	neglected	neglected

The compressor displacement volume is 18.46 cm^3; the expander displacement volume is 7.93 cm^3 at 3300 RPM for both devices.

The individual optimization is reported in Sections 6.4.1 to 6.4.3. The optimum designs of all mechanisms are compared in Section 6.4.4.

6.4.1 Reciprocating Piston

The reciprocating piston compressor and expander are assumed to each have two cylinders. The clearance volume is approximated by a distance between the piston and cylinder head of 1 mm at TDC. Given a fixed displacement volume, the geometry of a cylinder is a function of one variable, for instance the ratio of cylinder height to diameter. In addition to the aspect ratio of the cylinder, the performance is also affected by the cross sectional area of the inlet and outlet ports. It is assumed that a given fraction of the bore area is available as valve area. The area of the valve connecting to the high-pressure reservoir is 2/3 of the area of the low-pressure valve.

Sealing is provided by piston rings. The flow resistance of the piston rings is assumed equivalent to a flow passage of 3 mm length and 10 μm height per unit width. The shell pressure in both the compressor and expander simulation is the low-side pressure.

Compressor

Figure 21 shows the indicated and volumetric efficiency of a reciprocating piston compressor over a range of aspect ratios. The graphs show the effect of valve area on the performance. The indicated efficiency increases sharply from small aspect ratios, undergoes a maximum at aspect ratios on the order of 0.5 and reduces slowly at ratios greater than 0.5 to 1. This curve reflects the effects of leakage and valve losses on performance. At small aspect ratios, the area available for valves is small, so that the process is dominated by valve losses. As the bore area increases, the valve losses become

less important, but the sealing length around the piston increases, resulting in higher leak flow rates.

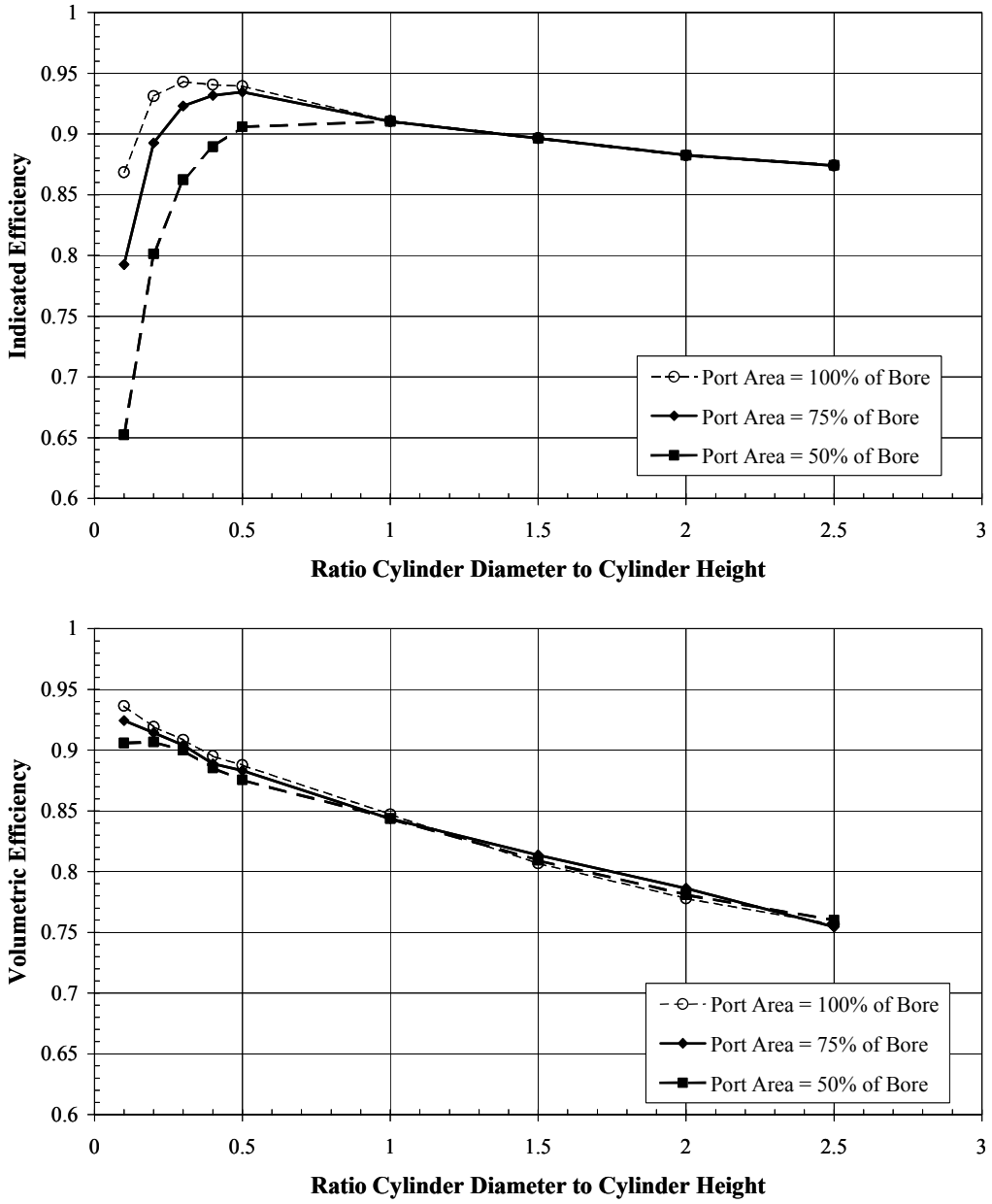

Figure 21: Performance of reciprocating piston compressor

In a realistic machine, the effective port area is probably in the range of 50% of the bore area. For this design, the optimum aspect ratio is in the order of 1. The resulting indicated efficiency is approximately 91% and the volumetric efficiency 84%. The bore and stroke of each cylinder are approximately 2.3 cm.

Expander

Figure 21 shows the indicated efficiency of a reciprocating piston over a range of aspect ratios. The graphs show the effect of valve area on the performance. The volumetric efficiency is not shown because it cannot be used to characterize the performance.

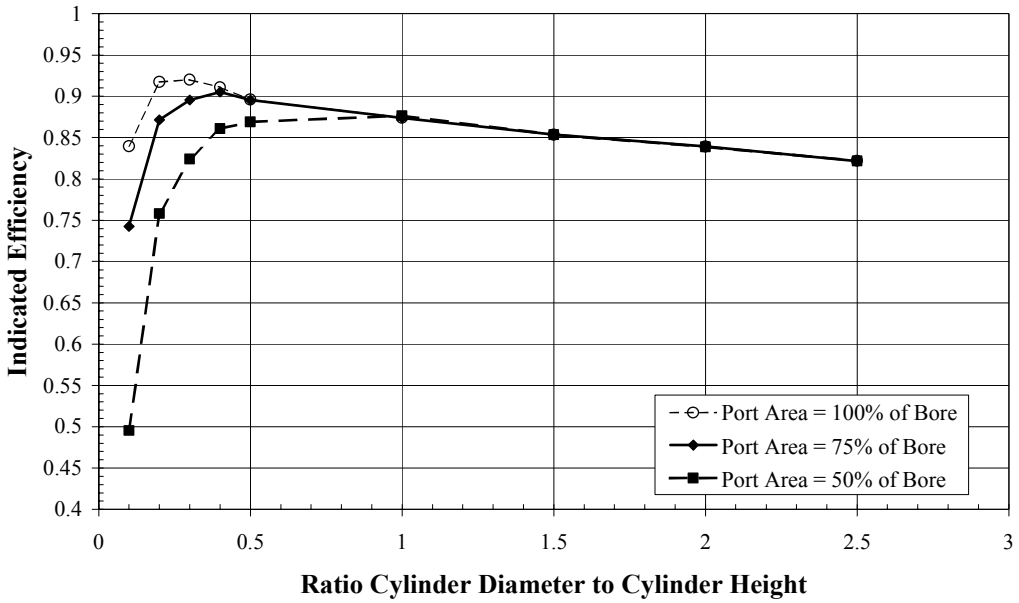

Figure 22: Performance of reciprocating piston expander

Assuming a port area in a realistic expander in the order of 50% of the bore area, the optimum aspect ratio is approximately 1. The resulting indicated efficiency is approximately 88%. The bore and stroke of each cylinder are approximately 1.7 cm.

6.4.2 Rotary Piston

With a given displacement volume and assuming a constant vane thickness of 4 mm, the design of a rotary piston device is a function of two independent variables. The displacement volume can be expressed in terms of the ratio of cylinder height to cylinder diameter and of cylinder diameter to piston diameter. In the simulations, the gap height of the leak between piston and vane is 3 μm. The leakage gap height between roller and cylinder side and between roller and cylinder end plates is 10 μm. It is assumed that the inlet and outlet ports can be designed large enough that valve losses can be neglected. The diameters of both ports were set to 12 mm. The clearance volumes introduced by the ports are estimated as half the volume of a cone with cylindrical cross section. The diameter of the cross sections and the heights of the cones are given by the diameter of the ports. The fluid trapped in the clearance volumes is assumed to undergo sudden expansion or compression when the clearance volume opens to the control volume. The shell pressure of the compressor is set to the pressure in the discharge reservoir. The leakage mechanism is via oil (see Section 5.2.2). The shell pressure in the expander is the discharge (low-side) pressure of the expander. The leakage mechanism is refrigerant leakage.

Compressor

The indicated and volumetric efficiencies of a range of design for rotary piston compressors are shown in Figure 23. The maximum performance is found for a ratio of cylinder height to diameter of 0.4 and for the ratio of piston diameter to cylinder diameter as small as possible. The theoretical limit for this ratio is 0.5. However, in a realistic machine, the oscillating motion of the vane is often a limiting factor, so that the piston diameter should not be smaller than 70% of the cylinder diameter (following the design of existing rotary piston compressors for conventional refrigerants). With this limitation, optimum ratio of cylinder height to cylinder diameter is approximately 0.5. The indicated and volumetric efficiency of this design is approximately 90% and 92%.

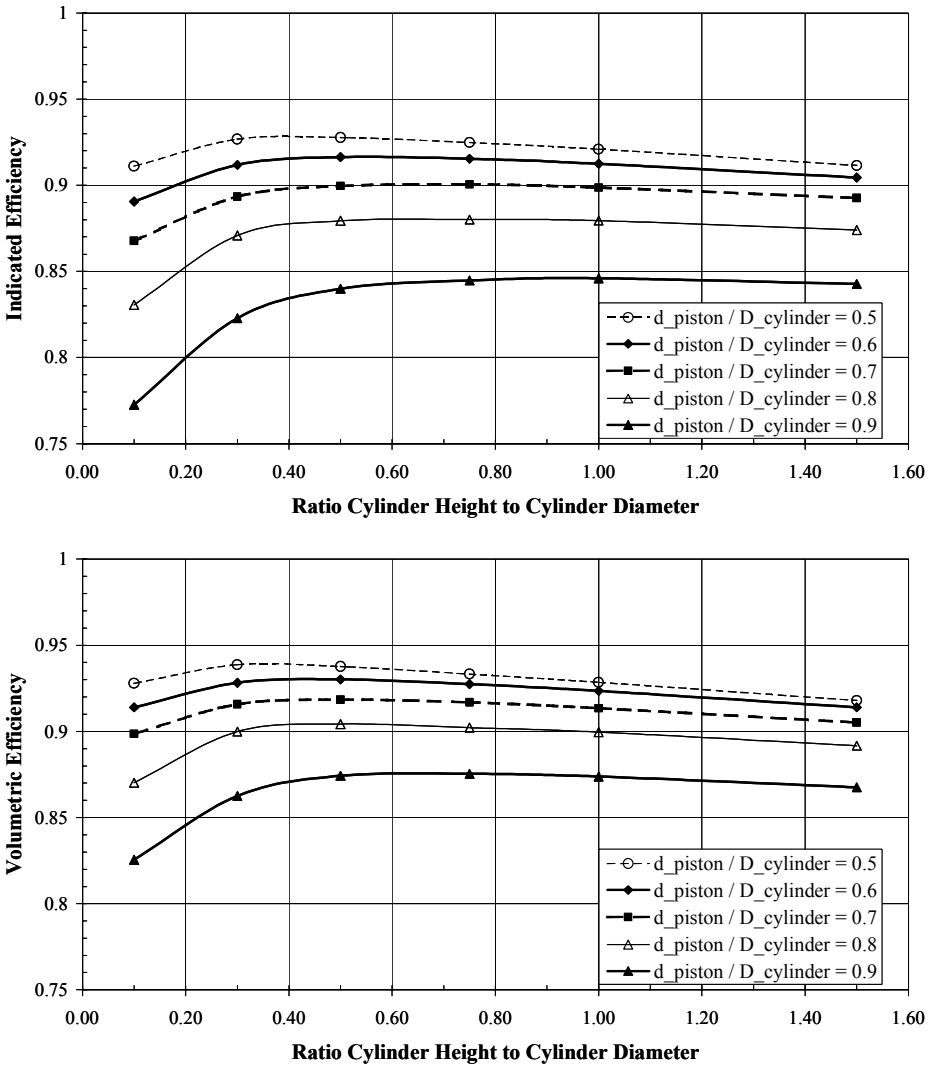

Figure 23: Performance of rotary piston compressor

The optimum cylinder diameter and height are approximately 4.9 cm and 1.9 cm, respectively. The piston diameter is approximately 3.4 cm.

Expander

The indicated efficiency of a rotary piston expander is shown in Figure 24 for a range of possible designs. The maximum performance is found at a ratio cylinder height to cylinder diameter of 0.3 and at a ratio cylinder diameter to piston diameter as small as possible. Choosing a minimum for the piston diameter of 70% of the cylinder diameter, the maximum indicated efficiency is approximately 87%. The resulting cylinder diameter and height are approximately 4.0 cm and 1.2 cm, respectively. The piston diameter is approximately 2.8 cm.

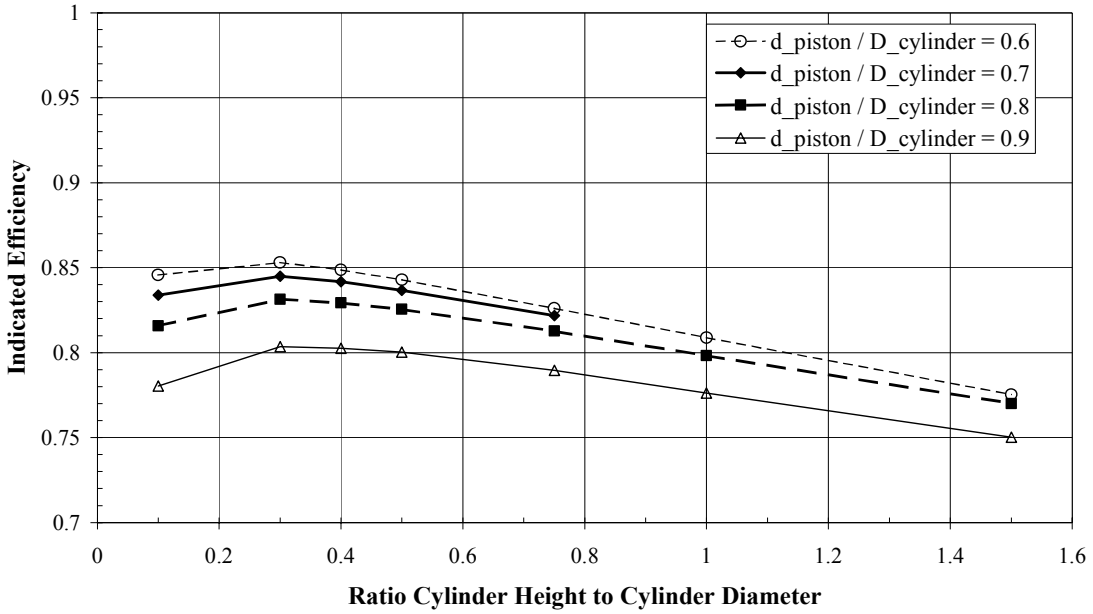

Figure 24: Performance of rotary piston expander

6.4.3 Scroll

The geometry of a scroll device is more complex than that of the piston devices discussed above. The milling tool method developed at CEEE (Lindsay and Radermacher 2000) allows an efficient and flexible description of the scroll geometry. The geometry is defined by the path of a circular milling tool through a block of material. The two scroll wraps are formed by the material remaining after the tool has moved from the side of the block to the center and outwards again (Figure 25 (a)). For simplification, the path of the milling tool is limited to an involute, and the tips of the scroll wraps are circular arcs in this project (Figure 25 (b)). The path of the milling tool at the center of the scroll is a straight line and the path outwards from the center is symmetrical to the first half of the path.

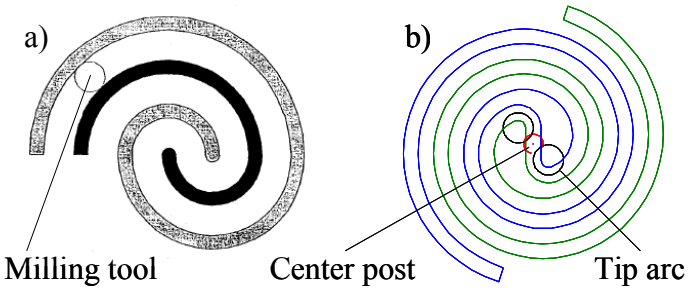

Figure 25: Milling tool method for scroll design

The scroll design is constrained by a given displacement volume and a given built-in volume ratio (for the compressor a minimum volume ratio is applied to avoid over-compression). The ratio of wall height to wall thickness should not exceed a value of 3.5 for material strength reasons (Preissner 2001) and the ratio of wall height and gap between two walls should be smaller than 2 in order to avoid deflection of the milling tool during machining. It is assumed that inlet and outlet ports can be designed large enough so that valve losses are insignificant. The leakage gap height for flank and tip leak was set to 10 μm.

With these limitations, the geometry of the scroll is a function of 6 variables with 4 constraints, for instance:

- Wall thickness
- Wall height
- Orbiting radius
- Tip radius
- Location of tip center
- String length of involute

Two constraints are equality constraints (displacement volume and volume ratio). The wall height and the length of the string of the involute are used to satisfy these constraints. The other two constraints are inequality constraints. A simple gradient search method is used to locate optimum designs. Starting from an initial design, the gradient of the performance as a function of the four independent variables is approximated. The method follows the direction of this gradient until either the performance decreases or a constraint is violated. If the performance decreases, a new gradient is approximated. If a constraint is violated, the method searches along this constraint in the direction of increasing performance. It is not guaranteed that this method finds a global maximum; therefore, the optimum design found may represent a local maximum.

It is assumed for both the compressor and expander simulation that suction and discharge are constant pressure processes. The shell pressure for both devices is the low-side pressure. The leakage mechanism is pure refrigerant leakage.

Table 5 lists the parameter of the optimum compressor and expander design. The indicated and volumetric efficiencies of the scroll compressor are 64% and 65%,

respectively. The indicated efficiency of the scroll expander is 75%. Figure 26 shows the shape of the wraps for optimum compressor and expander designs.

Table 5: Parameters of optimum scroll compressor and expander design

	Displacement volume [cm^3]	Volume ratio	Wall thickness [mm]	Wall height [mm]	Orbiting radius [mm]	Tip[2] x-coordinate [mm]	Tip radius [mm]	Overall diameter [mm]
Compressor	18.46	1.91	3.87	14.1	4312	5.2	3.83	82.5
Expander	7.3	2.42	2.7	9.3	2	-7.5	4.5	86.6

The performance of the expander is significantly better than the performance of the compressor. The reason is that the expander has a higher volume ratio, resulting in a longer wrap and more chambers in the scroll. Consequently, the pressure differences between chambers communicating through leaks, and hence the leak flow rates, are smaller.

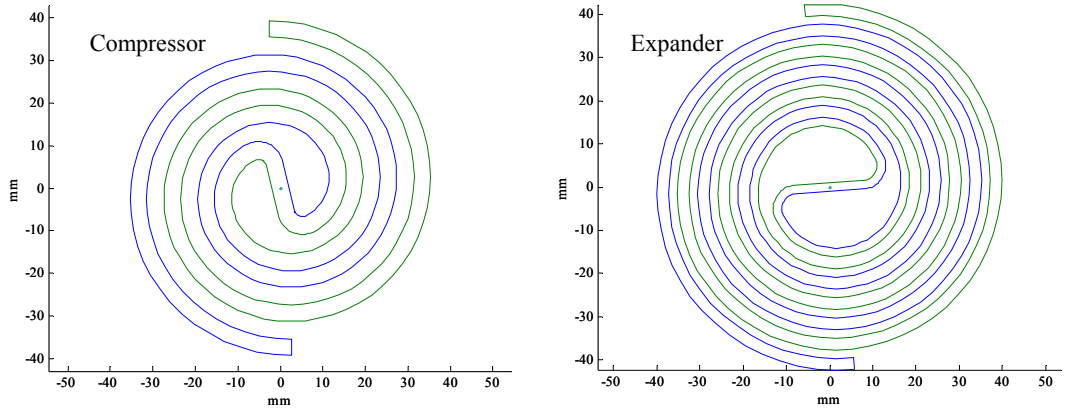

Figure 26: Optimum design for scroll compressor and expander

6.4.4 Comparison

The performance of the compressors and expanders over the pressure ratio is shown in Figure 27 to Figure 29. The leakage gap size for all devices is 10 µm. The boundary conditions (pressures and inlet densities) are in the range of expected values for an optimized expander cycle operating at ambient conditions from 32°C to 55°C. The cycle was simulated using constant values for the expander and compressor efficiencies. The built-in volume ratios of the expanders are not adjusted for the pressure ratio.

[2] The y-coordinate is determined by the milling tool method when reflecting the path of the tool at the center of the scroll.

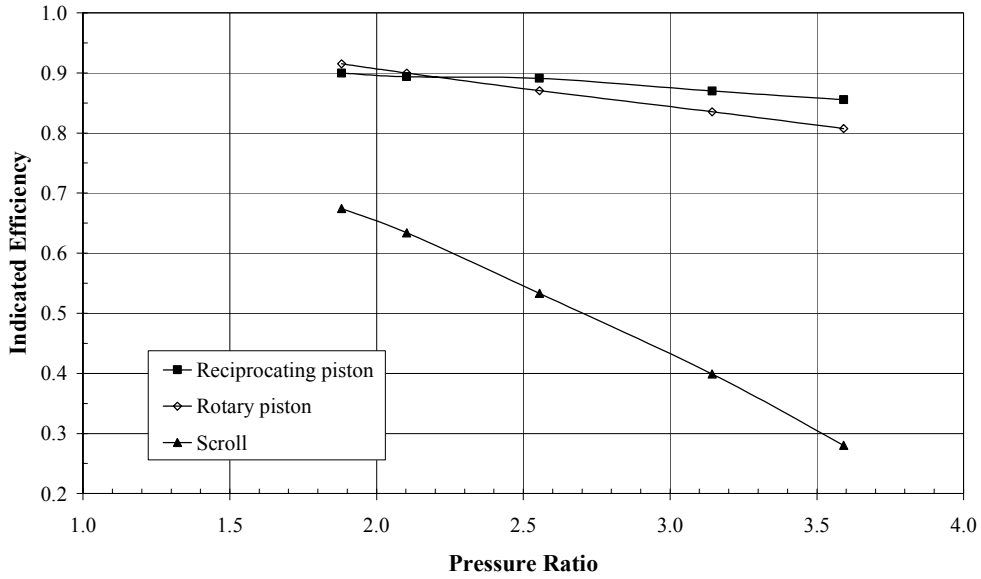

Figure 27: Compressor indicated efficiency vs. pressure ratio (leakage gap10 μm)

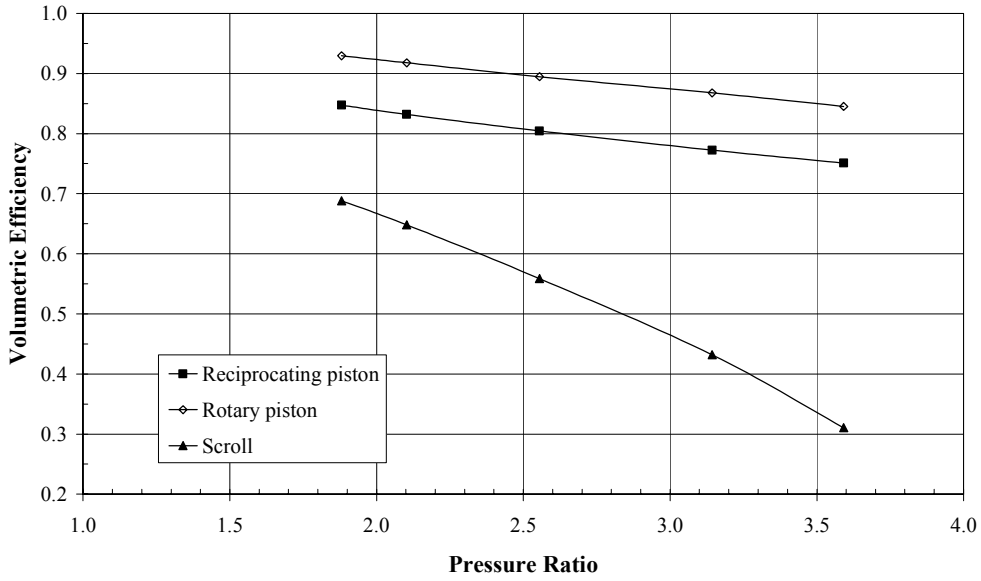

Figure 28: Compressor volumetric efficiency vs. pressure ratio (leakage gap 10 μm)

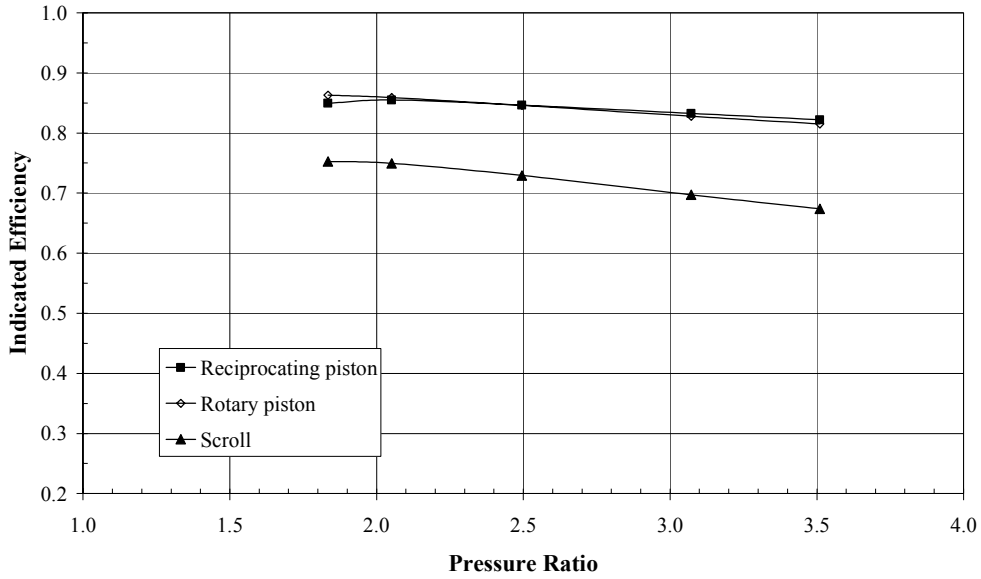

Figure 29: Expander indicated efficiency vs. pressure ratio (leakage gap 10 μm)

As found in the previous section, the scroll compressor performs significantly worse then the other mechanisms if no additional tip seal is used. Up to a pressure ratio of approximately 2.5, all compressors (except the scroll) have a similar performance. Above pressure ratios of 2.5, the performance of the rotary piston compressor falls behind that of the reciprocating. The reciprocating and rotary piston expanders perform similarly for all pressure ratios considered. The scroll expander performs 15% to 20% worse than the other expander mechanisms.

The performance of the devices has been evaluated for a range of machining tolerances. The results are shown in Table 6 and Table 7 and are plotted in Figure 30 through Figure 32. The reciprocating piston and rotary piston mechanisms perform similarly at all leakage gap sizes in the compressor and expander applications with the performance of the reciprocating piston dropping more with leakage gap size. The performance of the scroll compressor and expander drops sharply as the leakage gap size increases due to the large sealing length across the tip of the scroll wraps. For almost all conditions, the scroll performs worse than the other mechanisms analyzed. Only at very tight machining tolerances does the scroll expander perform better than the reciprocating piston expander.

Table 6: Compressor indicated and volumetric efficiency vs. leakage gap size

	5 μm		10 μm		15 μm	
	η_{ind}	η_{vol}	η_{ind}	η_{vol}	η_{ind}	η_{vol}
Recip piston	0.93	0.88	0.91	0.84	0.85	0.79
Rotary piston	0.96	0.96	0.90	0.92	0.85	0.87
Scroll	0.87	0.88	0.64	0.65	0.39	0.38

Table 7: Expander indicated efficiency vs. leakage gap size

	5 μm η_{ind}	10 μm η_{ind}	15 μm η_{ind}
Recip piston	0.90	0.87	0.81
Rotary piston	0.94	0.84	0.78
Scroll	0.93	0.75	0.47

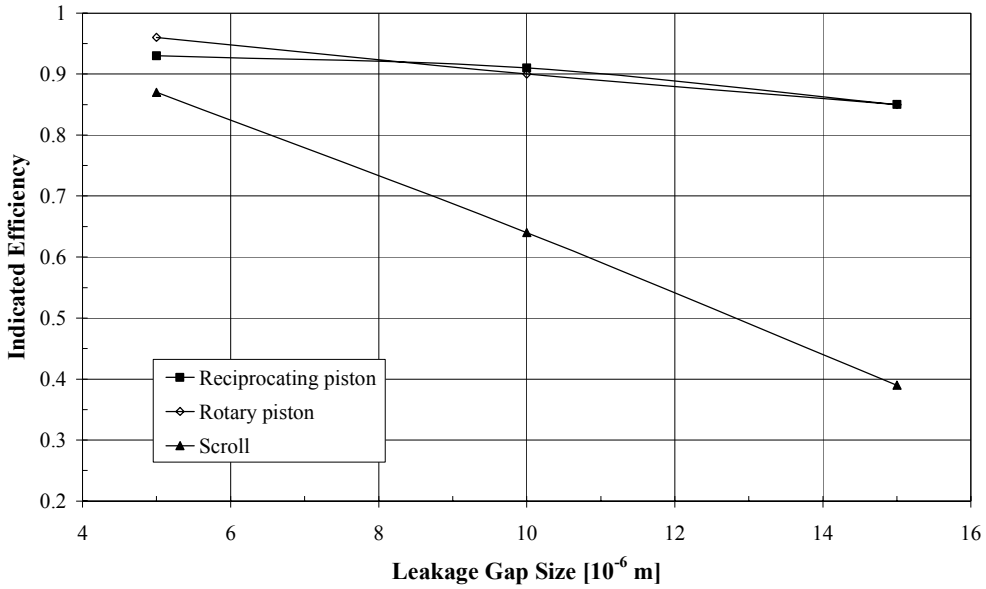

Figure 30: Compressor indicated efficiency vs. leakage gap size

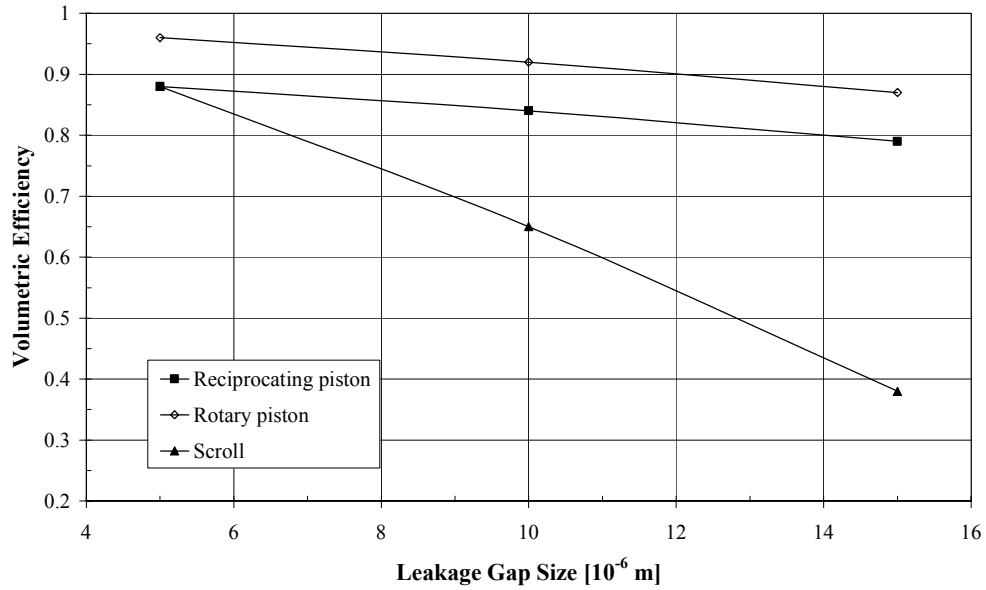

Figure 31: Compressor volumetric efficiency vs. leakage gap size

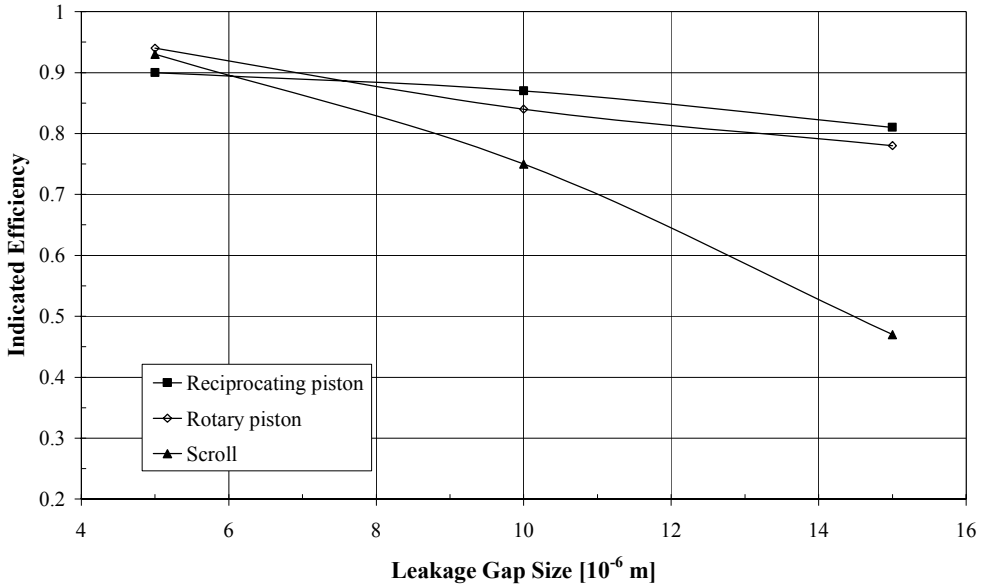

Figure 32: Expander indicated efficiency vs. leakage gap size

6.5 Discussion

The low performance of the scroll compressor and expander at higher leakage gap sizes implies a strong disadvantage of this mechanism compared to the others. This strong disadvantage is not found in scroll compressors for conventional refrigerants, due to smaller pressure differences compared to CO_2 and good sealing methods available. In order to fully explore the potential of the scroll mechanism as compressor and expander in a CO_2 system, accurate data about the effective leakage gap size as well as experimental investigations are necessary.

When analyzing the results of the expander optimization, it must be considered that all devices were simulated with ideal valve actuation. The assumption is not critical for the scroll expander, because opening and closing of the ports in these devices is purely dependent on the crankshaft angle. In the reciprocating and rotary piston expander however, the expansion compartment is permanently connected to the inlet and/or outlet port. Therefore, the timing of the port openings must be controlled externally.

For the reciprocating piston, both the inlet and the outlet port must be controlled. Heyl (2000) used valves actuated by pressurized air and Beak et al. (2002) used solenoid valves in CO_2 reciprocating piston expanders. In both of these projects, the expander speed was limited to approximately 60 RPM due to valve timing. Heidelck and Kruse (2000) investigated rotating disc with slots as control mechanisms, borrowed from hydraulics applications. It has the advantage of the valve control depending only on the shaft speed and not on external means. Heidelck and Kruse report that a first prototype showed problems with leakage through the valves.

For the rotary piston expander, only the inlet port needs to be controlled. When operated at the same shaft speed, the inlet port of a rotary piston expander is open twice as long as the port of a reciprocating piston expander, potentially reducing the problems with externally controlled valves. It may also be possible to adopt the concept of a rotating disc as valve control for the rotary piston expander.

The small variation of the expander indicated efficiency over the pressure ratio (Figure 29) indicates that it may not be necessary to adjust the built-in volume ratio to the operating conditions over the range considered here. The volume ratio over the range of ambient conditions between 32°C and 55°C changes from approximately 2.3 to 2.9. The performance degradation for a volume ratio mismatch on the order of 25% can be estimated from Figure 5. The indicated efficiency drops by approximately 5%.

The gas trapped in the clearance of the reciprocating and rotary piston compressors undergoes re-expansion until the pocket pressure is close to the pressure in the suction line. In the reciprocating and rotary piston expanders however, the inlet valve opens when the pocket volume begins to increase. The gas in the clearance volume is at low pressure and low density. The incoming gas is high-pressure, high-density gas. In the first instants after the inlet valve opens, the suction gas undergoes sudden, irreversible expansion until the pressure level in the pocket reaches the pressure in the high-pressure line. This process introduces additional losses in the expansion process in the piston devices. It is theoretically possible to eliminate these losses with accurate valve timing.

The inlet and outlet ports of the scroll compressor uncover at specific angles of the crankshaft without need of external actuators. However, without additional control, a scroll expander operates with constant volume ratio, which does not necessarily match the optimum volume ratio imposed by the boundary conditions. The volume ratio of a scroll compressor is usually adjusted by a reed valve after the discharge port, so that the center pocket of the scroll opens to the discharge reservoir only when the pocket pressure has reached the reservoir pressure. In a scroll expander, the port at the center of the scroll is the inlet port. The use of a reed valve for the timing of the port is not possible. An external control is necessary to adjust the built-in volume ratio to the operating conditions.

The built-in volume ratio in screw compressors can be adjusted by a slide vane controlling the axial discharge port (variable Vi, Shaw 1988). It may be possible to use a similar mechanism for the slide valve in a scroll compressor. The technology for the actuation of the valve is already developed. Nippon Soken and Denso (1997) developed a control valve for a CO_2 cycle with isenthalpic expansion valve, which adjusts the high-side pressure to the optimum value depending on the operating conditions. This valve does not require an external control.

While the low volumetric efficiency of the reciprocating piston compressor is due to the large clearance volume in this device, the low volumetric efficiency of the scroll compressor is due to leakage and indicates real losses. Comparing the results of the scroll

compressor and expander indicates that the compressor performance may be improved by using a design with longer wraps to reduce driving pressure differences across the leaks. However, this option was not found in the optimization of the compressor. The optimization algorithm moved the design more in the direction of short wraps and high wall thickness. This means leakage in the compressor can best be reduced by increasing the flow resistance in the leaks (rather than reducing the driving force as in the expander). Therefore, it may be advantageous to deviate from the involute design to more advanced geometries, for example the two-turn scroll presented by Lindsay and Radermacher (2000).

The effect of friction has not been included in these simulations. The losses due to friction depend on the mechanisms as well as the specific design within each mechanism. More detailed simulation is necessary in order predict the performance of a compressor or expander including the effect of friction.

The first experimental results of the performance of a semi-hermetic reciprocating piston CO_2 compressor indicate that the isentropic efficiency is approximately 15% lower than the indicated efficiency (Neksa et al.1999). To obtain an approximation for the isentropic efficiency of other compressor types and expanders, it is assumed that all devices dissipate a constant amount of energy through friction and other losses. Using the published data for the semi-hermetic CO_2 compressor as a baseline, the work dissipated in the devices is determined such that the isentropic efficiencies of the reciprocating type devices with a leakage gap size of 10μm is 15% below the respective indicated efficiencies at the relevant operating conditions. The isentropic efficiencies for the compressor and expander, respectively, can then be written as:

$$\eta_{is} = \frac{W_{is}^{Comp}}{W_{is}^{Comp} + x_{Comp} \cdot W_{is}^{Comp}} \quad Compressor$$

$$\eta_{is} = \frac{W_{is}^{Exp} - x_{Exp} \cdot W_{is}^{Exp}}{W_{ind}^{Exp}} \quad Expander$$

Equation 37

where x_{Comp} and x_{Exp} are fractions of the isentropic work of the compressor and expander, respectively, which are adjusted to achieve the desired results. Table 10 and

Table 11 list the values of the isentropic efficiencies for the different compressor and expander types at the range of leakage gap sizes considered.

Table 8: Compressor isentropic efficiency vs. leakage gap size

	5 μm η_{is}	10 μm η_{is}	15 μm η_{is}
Recip piston	0.77	0.76	0.72
Rotary piston	0.79	0.75	0.72
Scroll	0.73	0.56	0.36

Table 9: Expander isentropic efficiency vs. leakage gap size

	5 μm η_{is}	10 μm η_{is}	15 μm η_{is}
Recip piston	0.75	0.72	0.66
Rotary piston	0.79	0.69	0.63
Scroll	0.78	0.60	0.32

7 INTEGRATION CONCEPTS

To minimize energy conversion losses the expander work should be directly utilized as mechanical work input to the compressor. The integration of the expander work in the cycle reduces the need for energy storage because the energy supply from the expander always coincides with the energy demand from the compressor. In order to reduce coupling and gear losses, the compressor and expander should be connected through a common shaft (Figure 33).

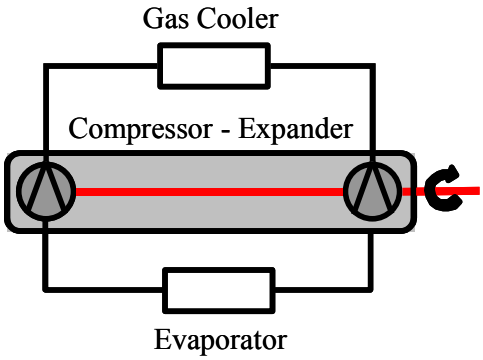

Figure 33: System with integrated compressor–expander

The concept of direct mechanical coupling is generally possible with all the displacement mechanisms analyzed in this report. Heyl (2000) has demonstrated this concept for a reciprocating piston compressor–expander and Smith et al. (1995) for an integrated screw device (Expressor) (CITY 2002).

With the expander coupled directly to the compressor shaft, the control of the high-side pressure requires special attention. Different from sub-critical cycles, the transcritical cycle with CO_2 as refrigerant has an optimum high-side pressure at which the COP reaches a maximum at given ambient conditions. In a CO_2 cycle with an isenthalpic expansion valve, the optimum high-side pressure is adjusted by the expansion valve setting. In a cycle with an expander, the high-side pressure can be optimized by adjusting the mass flow rate through the expander (assuming constant compressor speed and displacement volume). The expander mass flow rate can be varied by the expander speed or displacement volume. In a cycle with an integrated compressor–expander, the expander speed cannot be adjusted independently of the compressor speed. This means in a system with integrated compressor–expander (Figure 33), the expander mass flow rate can only be modified with a variable expander displacement volume. Another option is to introduce an additional expansion valve into the cycle, which can be operated independently from the compressor and expander.

Figure 34 shows block diagrams of possible circuitries, which can control the high-side pressure independently from the compressor shaft speed.

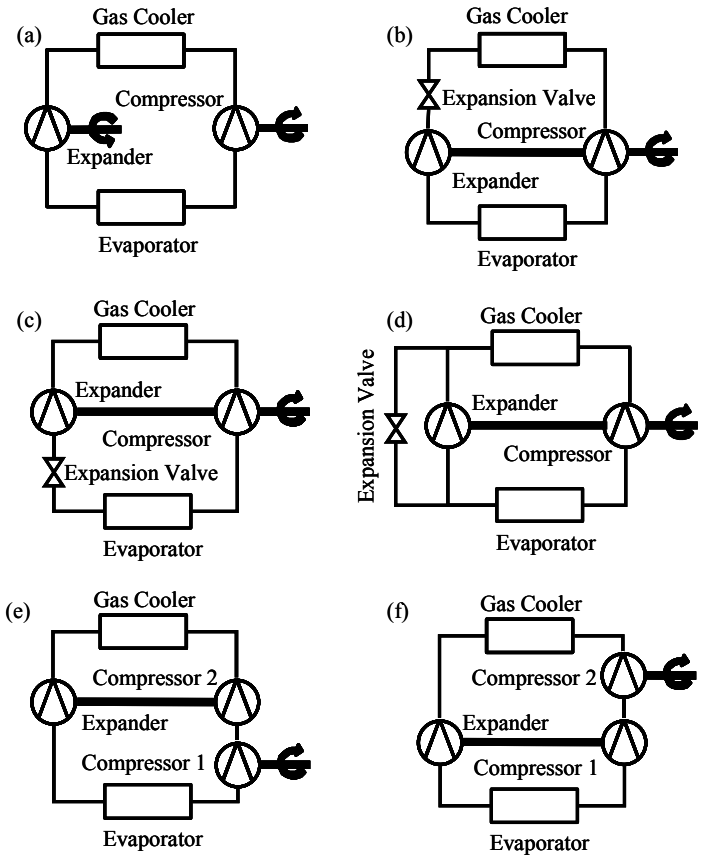

Figure 34 : Circuitry options for high-side pressure control in expander systems

Option (a) in is a system with independent compressor and expander speeds. In options (b) and (c), the high-side pressure may be adjusted by increasing the total flow resistance across the expansion section by introducing an additional, adjustable pressure drop. Option (c) adjusts the flow resistance across the expansion section by introducing an adjustable by-pass to the expander. In options (e) and (f), the compression is divided into two sections. The expander speed is determined by the operating conditions. The low-stage compressor (e) or the high-stage compressor (f) is independent of the expander speed. Option (f) is patented by Sanden and has been investigated experimentally by Heyl and Quack (2000). The expander used therein had an isentropic efficiency of 51% and the system COP was improved by 30% compared to the two-stage system without expander. Due to problems with valve operation, the expander was operated with a full-pressure stroke, and only the flow work of the process was utilized. Option (f) offers the possibility of placing the expander and the low-stage compressor close to the evaporator inlet, so that the heat transfer to the refrigerant in the liquid line is minimized, resulting in higher capacity. With the first compression stage close to the evaporator outlet, the heat transfer to the refrigerant can be reduced, minimizing the suction heating to the high-stage compressor and reducing the discharge temperature. A lower discharge temperature reduces the compressor work and the heat load that must be rejected in the gas cooler.

7.1 Performance Analysis

The circuitries (a) to (f) in Figure 34 have been analyzed assuming the following simplifications:

- Constant volumetric and isentropic efficiency of compressor and expander
- Constant UA value for heat exchangers
- Saturated vapor at evaporator outlet
- Energy balance, mass balance, and heat transfer determine high-side and low-side pressure

For each circuitry or option, the appropriate control parameter was varied in order to investigate its feasibility to control the high-side pressure.

Figure 35 shows results of the simulation of option (a), expander speed independent from compressor speed. The P-h diagram (B) shows three cycles with different expander speeds. This option allows adjusting the high-side pressure. The COP undergoes a maximum as the expander speed varies (C).

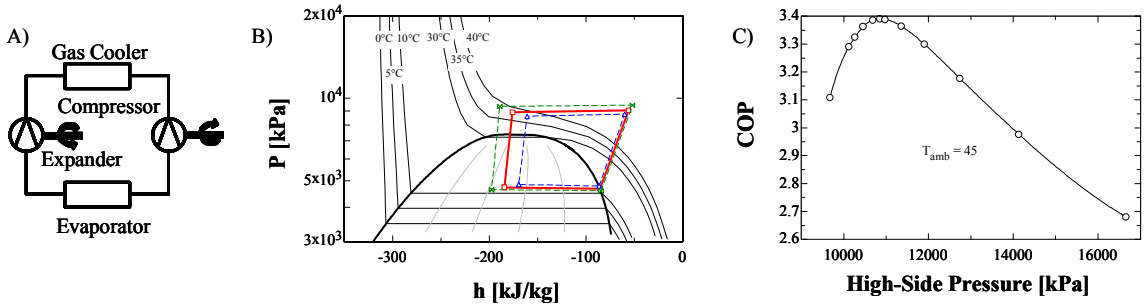

Figure 35 : High-side pressure control with independent expander speed

Figure 36 shows the results for option (b), adjustable expansion valve upstream of expander. The P-h diagram (B) shows the cycle without expansion valve (solid) and with expansion valve (dashed). The flow restriction of the expansion valve has almost no effect on the high-side pressure. The plot (C) shows the performance of the system and the performance of the system with independent compressor and expander. The system for option (b) is designed such that the high-side pressure is approximately 1000 kPa below the optimum pressure with the expansion valve fully open. As the expansion valve opening is reduced, the high-side pressure is expected to increase. However, the graphs show that the pressure changes insignificantly. The COP does not reach a maximum, but decreases constantly as the flow restriction is increased. This means that option (b) cannot be used to control the system.

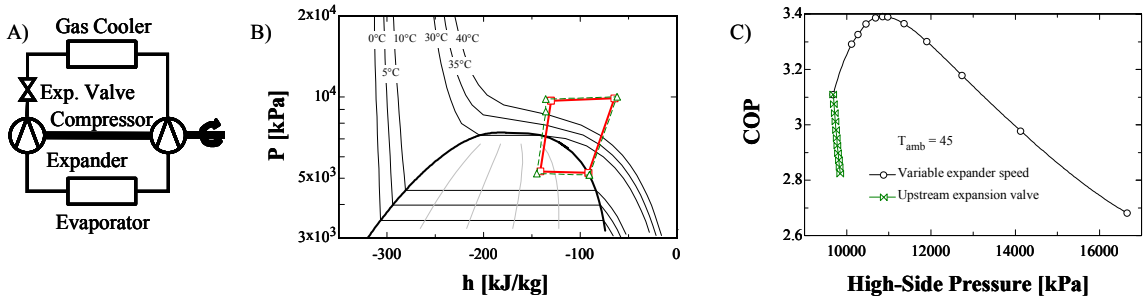

Figure 36 : High-side pressure control with expansion valve before expander

Figure 37 shows the results for option (c). The findings are similar to the ones for option (b). The expansion valve opening has no distinguishable effect on the high-side pressure (plot B) and the COP cannot be optimized (plot C). Thus circuitry (c) is not a viable option for controlling the system.

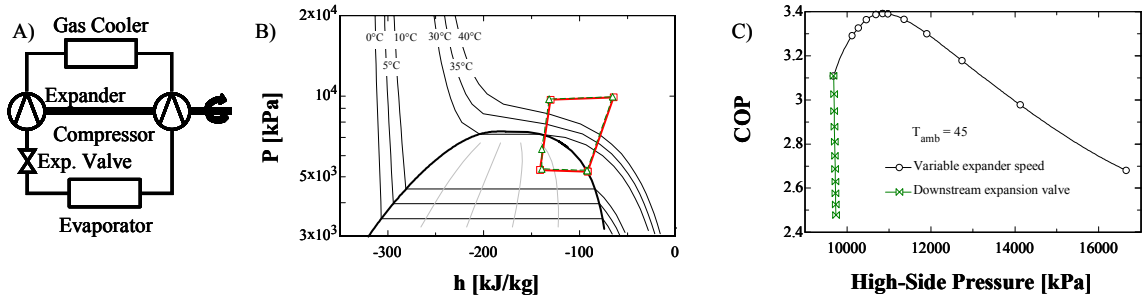

Figure 37 : High-side pressure control with expansion valve after expander

Figure 38 shows the results for circuitry (d). The by-pass to the expander allows only reducing the high-side pressure. The system is designed such that high-side pressure is approximately 3000 kPa above the optimum pressure when the by-pass is closed. As the expansion valve is opened, the high-side pressure decreases (plot B) and the COP undergoes a maximum (plot C). However, the maximum found with this circuitry is significantly below the performance found with compressor and expander operated independently. Thus, this circuitry cannot be considered an appropriate option for the system control.

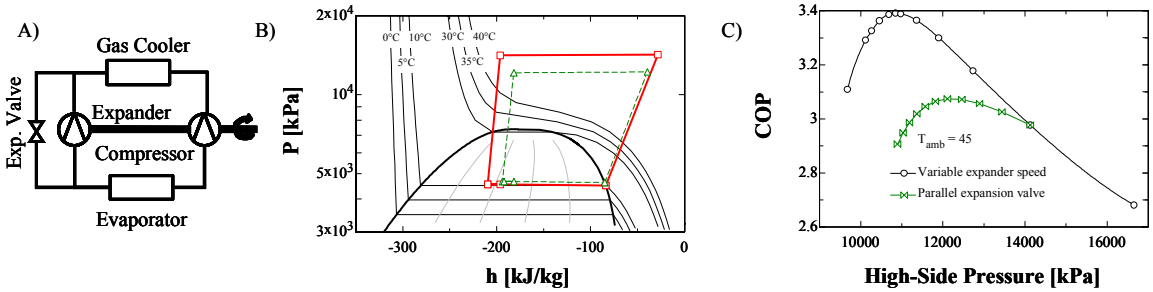

Figure 38 : High-side pressure control with by-pass valve

The by-pass to the expander can be interpreted as controlled internal leakage in the device. Revisiting the results of the simulation implies that there is an “optimum” leak

flow rate (greater than zero) for the expander if the compressor and expander speeds are coupled and the system operates off the optimum expander speed. The expansion valves before and after the expander can be interpreted as adjustable valve losses at the expander inlet and outlet. Accordingly, the results make sense, since the performance is expected to drop as the valve losses increase.

The results of the analysis show that the expander speed is the only acceptable control variable in the expander systems considered. Figure 39 shows the performance of the system with independent expander speed versus high-side pressure and versus the expander speed for a range of gas cooler air temperatures.

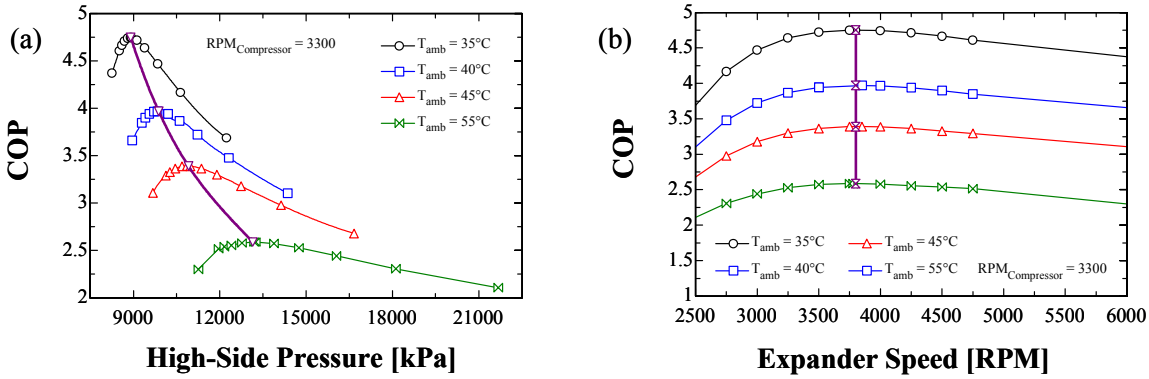

Figure 39: (a) COP vs. high-side pressure and (b) vs. expander speed

For all air temperatures considered, the maximum COP occurs at the same expander speed. Since the compressor speed was kept constant, this result implies that the optimum ratio of compressor speed to expander speed is constant over the range of operating conditions considered (gas cooler air inlet temperature 35°C to 55°C, evaporator air inlet temperature 27°C at 50 relative humidity). Hence, the displacement volumes of the devices can be designed such that the ratio of speeds is equal to unity and the compressor and expander can be operated with the same speed.

Figure 40 shows the system performance for various values of the compressor speed for a range of gas cooler air temperatures. The graphs show that the system can be operated close to the maximum COP for all operating conditions considered with a constant ratio of compressor speed to expander speed, if the ratio is chosen appropriately. The lines for constant ratio of compressor RPM to expander RPM indicate the same ratio in all graphs. The COP is within 3% of the maximum COP at the respective operating point. This means that it may be possible to design the system such that no additional control for the high- side pressure is necessary even if the speed of the integrated device is varied.

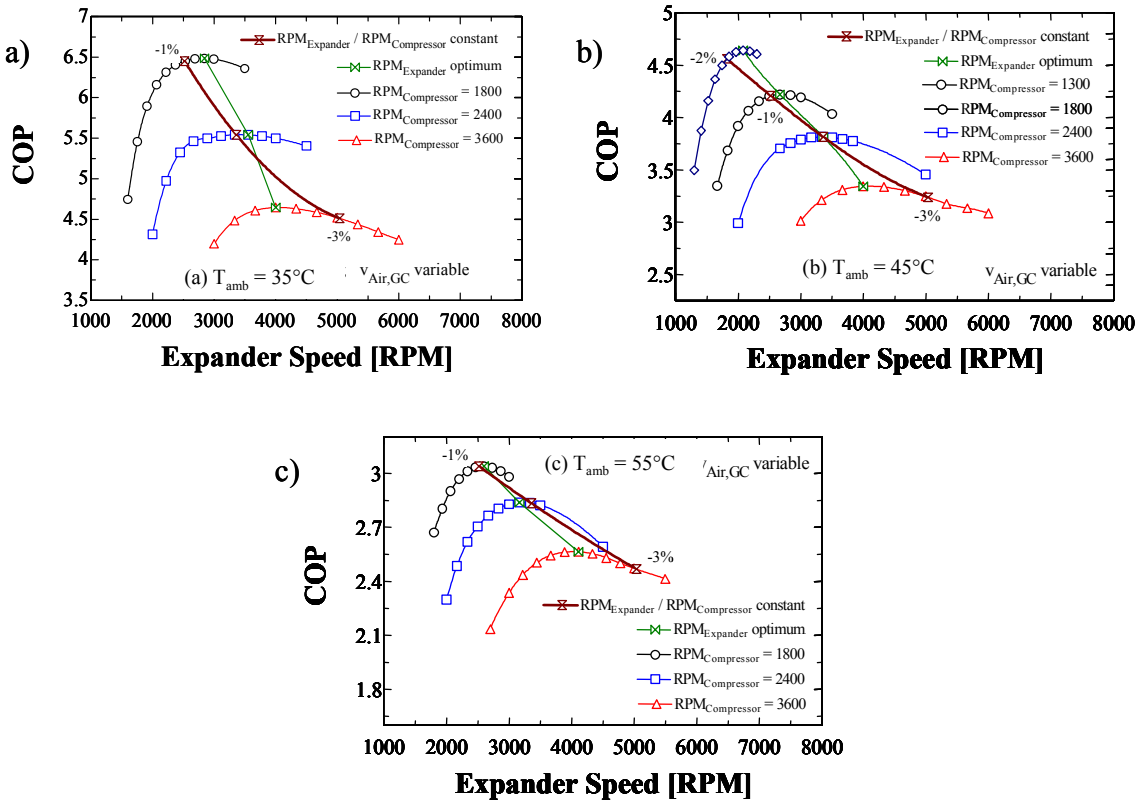

Figure 40: COP vs. expander speed of directly coupled system for range of compressor RPM and gas cooler air temperatures

8 SUMMARY AND CONCLUSIONS

Performance Potential of CO_2 Systems with Expander

An ideal expander can improve the energy efficiency of a transcritical CO_2 system under typical residential A/C operating conditions of ambient temperatures between 28°C and 50°C by 41% to 81%, respectively. Simulation results are shown in Figure 41. With an expander of 80% efficiency, the system performance can be improved by 31% to 56% and with an expander of 60% efficiency by 22% to 38%, at ambient temperatures between 28°C and 50°C, respectively. Compared to a conventional R22 system, the energy efficiency of a CO_2 system with an ideal expander is higher at all ambient temperatures considered. With an 80% efficient expander, the CO_2 system performs better than a conventional R22 system at ambient temperatures below 36°C. At 28°C, the CO_2 system performs 22% better and at 50°C, it performs 11% worse. A CO_2 system with an expander of 60% efficiency operates 13% more energy efficiently than the R22 system at ambient temperatures of 28°C and 21% less energy efficiently at ambient temperatures of 50°C. At approximately 31°C, both systems operate with the same energy efficiency.

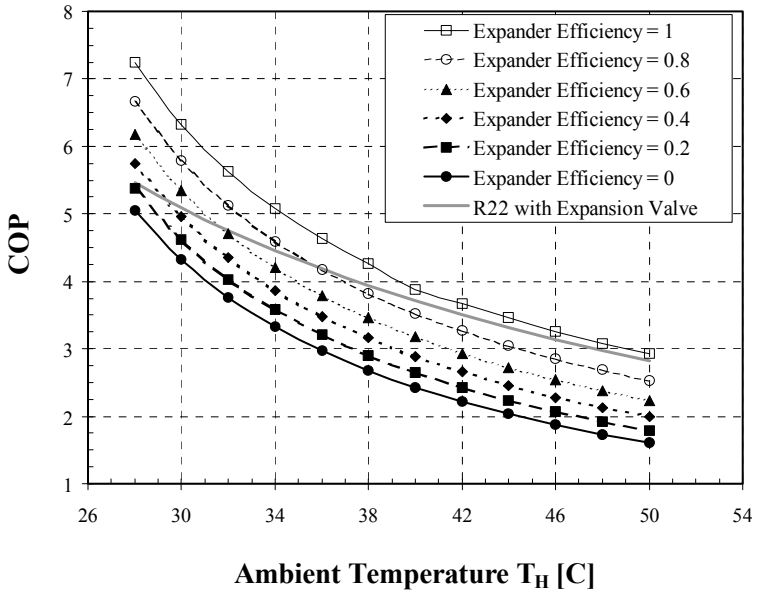

Figure 41: Performance of CO_2 expander system and conventional R22 system

Under most operating conditions, the performance of a CO_2 expander system does not benefit from a suction line heat exchanger. Although the SLHX increases the specific cooling capacity, it also reduces the expander work output and increases the compressor work input. If more than 30% of the expander work output can be recovered, the SLHX does not benefit the system performance. However, when designing a system, other factors than the energy efficiency may influence the decision regarding the integration of an SLHX.

Analysis of Expander and Compressor Performance

The performance of expanders and compressors depends on irreversible processes during the expansion/compression process. The dominating irreversibilities in positive displacement machines are:

- Internal leakage
- Valve losses
- Over/under compression/expansion
- Internal heat transfer

Internal heat transfer has a negligible effect on the performance of a compressor in a residential size CO_2 air-conditioning system. In an expander for this type of application, internal heat transfer can affect the performance significantly due to the increased heat transfer coefficient during evaporation. At adiabatic operating conditions, i.e. when the net heat transfer between fluid and expander wall is equal to zero, internal heat transfer affects the expander performance by less than 3%. An integrated compressor–expander device operates adiabatically when the net heat transfer between compressor and expander is equal to zero. The heat transfer is dominated by the expander. Therefore, the adiabatic operating point of the integrated device is close to the adiabatic operating point of the expander alone. Hence, the effect of internal heat transfer on the performance of an integrated device is in the order of a few percent and is thus neglected in the simulations.

The performance of three positive displacement mechanisms as expander and compressor in a CO_2 system has been analyzed considering the losses mentioned above:

- Reciprocating piston
- Rotary piston
- Scroll

Tables 8 and 9 list the expected performance of the mechanisms with optimized geometry at ASHRAE A operating conditions depending on the leakage gap size. For all simulations, the valve timing was assumed ideal for all devices

Table 10: Compressor indicated, isentropic, volumetric efficiency vs. leakage gap size[3]

	5 µm			10 µm			15 µm		
	η_{ind}	η_{is}	η_{vol}	η_{ind}	η_{is}	η_{vol}	η_{ind}	η_{is}	η_{vol}
Recip. piston	0.93	0.77	0.88	0.91	0.76	0.84	0.85	0.72	0.79
Rotary piston	0.96	0.79	0.96	0.90	0.75	0.92	0.85	0.72	0.87
Scroll	0.87	0.73	0.88	0.64	0.56	0.65	0.39	0.36	0.38

[3] For the isentropic efficiency assumptions, see Section 6.5, p. 40

Table 11: Expander indicated and isentropic efficiency vs. leakage gap size[4]

	5 μm		10 μm		15 μm	
	η_{ind}	η_{is}	η_{ind}	η_{is}	η_{ind}	η_{is}
Recip. piston	0.90	0.75	0.87	0.72	0.81	0.66
Rotary piston	0.94	0.79	0.84	0.69	0.78	0.63
Scroll	0.93	0.78	0.75	0.60	0.47	0.32

The reciprocating piston and rotary piston mechanisms perform similarly at all leakage clearances. The performance of the scroll mechanism is the most dependent on the leakage gap size. At machining tolerances above 5 μm, the scroll mechanism performs significantly worse than the other mechanisms. The performance of the scroll mechanism is dominated by the leakage across the tips of the scroll wraps. If this leakage path is eliminated, the indicated efficiency of a scroll expander, for instance, is above 90% for a flank clearance of 15 μm.

Figure 42 shows the indicated compressor and expander efficiency over the range of pressure ratios at typical A/C operating conditions.

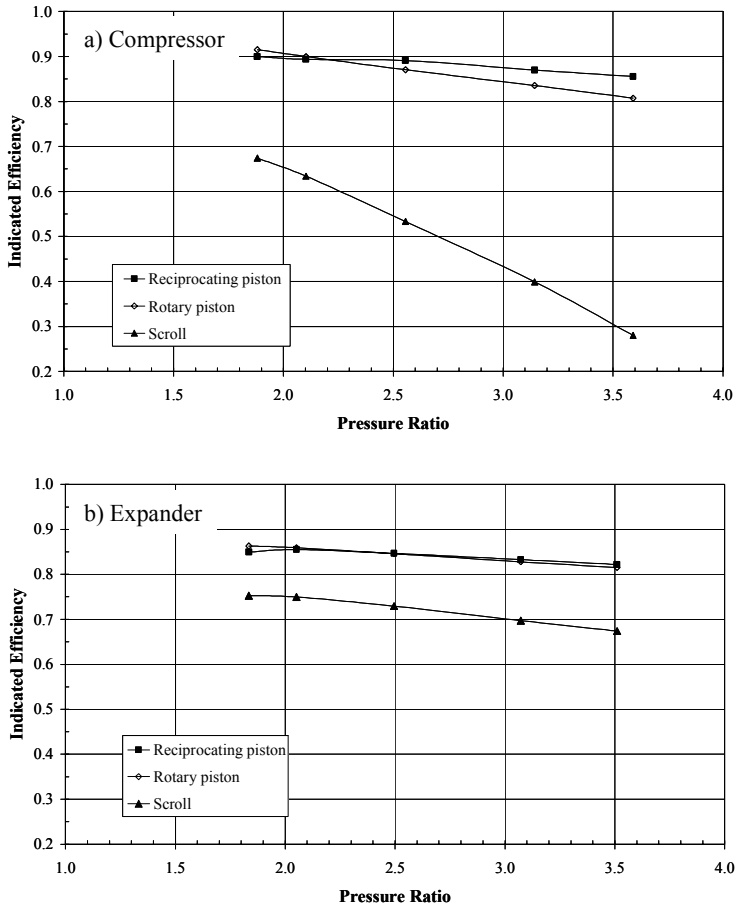

Figure 42: Compressor (a), expander (b) indicated efficiency vs. pressure ratio (leakage gap 10μm)

[4] For the isentropic efficiency assumptions, see Section 6.5, p. 40

The piston compressors perform similarly over the range of pressure ratios. The performance of the rotary piston compressor falls behind that of the reciprocating piston compressor at higher pressure ratios. The scroll mechanism performs poorer as compressor than the other mechanisms. As in the expander application, the mechanism is dominated by leakage across the tip of the scroll wraps. If this leakage path can be reduced, the scroll could perform similarly to the other mechanisms. Experience with scroll compressors for conventional refrigerants indicates that efficient sealing mechanisms are available.

The valve operation for the two piston type expanders requires special attention. Since it is not possible to use reed valves in an expander application, externally controlled valves must be used for these mechanisms. Previous experiments with reciprocating piston expanders revealed that the valve control might be a major challenge. If the volume ratio is optimized for one operating condition and not adjusted for others, the losses due to over/under expansion are in the range of 10% of indicated efficiency at typical A/C operating conditions.

The effect of friction was not considered in the simulation. The losses due to friction depend on the type of device and the individual design of the machine. Detailed research on the individual design level is necessary to reliably predict the performance potential of a specific machine.

Integration Concepts

In order to efficiently utilize the work produced by the expander, the compressor and expander should be integrated on a common shaft. With this design, the adjustment of the high-side pressure to the operating conditions requires special attention. Since the expander speed is coupled to the compressor speed, the high-side pressure cannot be adjusted by the expander RPM. The system cannot be controlled by an additional expansion valve in series or in parallel to the expander. However, the system can be operated at or close to the optimum performance over the range of typical A/C operating conditions (ambient temperature between 30°C and 50°C, evaporating temperature 7°C) at constant ratio of compressor speed to expander speed if compressor and expander displacement volumes are designed appropriately. Simulation shows that this control concept is also applicable for integrated devices with variable speed.

Expected Performance of Residential CO_2 Air-Conditioning System with Expander

Assuming an effective leakage gap size of 10 μm, the indicated efficiency of a reciprocating piston compressor is in the order of 91% and the indicated efficiency of a reciprocating piston expander is in the order of 87% at ambient temperatures of 28°C to 50°C. Additional losses due to bearing friction, suction heating, and entrance and exit effects to the compressor/expander shell reduce the expander efficiency by approximately 15% below the indicated efficiency. With this estimation, the isentropic efficiency of the compressor is approximately 76% and the isentropic efficiency of the expander is approximately 72%. The resulting COP of an expander system is 6.6 at 28°C ambient

temperature and 2.4 at 50°C ambient temperature. At 28°C, the CO_2 expander system performs 20% more energy-efficiently than a conventional R22 system. At 50°C, the CO_2 system performs 14% less energy-efficiently than the R22 system. At approximately 34°C, both systems perform with the same energy efficiency.

APPENDIX A

Modeling Assumptions for the Comparison of CO_2 and R22

Both systems are simulated with constant cooling capacity, independent of the operating conditions. For both systems, the evaporator pressure is assumed to be an independent variable, fixed for all operating conditions. The evaporating temperature is assumed to be 0 – 2K higher in the CO_2 systems than in the R22 system, reflecting the potential of superior heat transfer properties of CO_2. The evaporating temperature in the R22 system is 9°C and in the CO_2 system 9°C - 11°C. The refrigerant leaves the evaporator as saturated vapor for all cases in both systems. Unless otherwise stated, the evaporator secondary fluid is air with 27°C inlet temperature and 50% relative humidity. The compression is assumed adiabatic with constant isentropic efficiency. The isentropic efficiency for the R22 compressor is 0.7 and for the CO_2 compressor slightly higher at 0.75. The higher efficiency of the CO_2 compressor is due to a smaller pressure ratio across the compressor (Preissner 2001, Sakamoto and Giese 2000). The condensation temperature in the subcritical cycle is assumed to be 12K above the air inlet temperature and the refrigerant leaves the condenser with a sub-cooling of 8.6K. The gas cooler outlet temperature in the CO_2 system is set to 2.5K above the air inlet temperature. The high-side pressure is optimized for each operating condition. The refrigerant pressure drop in the gas cooler/condenser is constant in both systems at 100 kPa. The pressure drop in the evaporator of the subcritical R22 system is 25 kPa and in the CO_2 system 50 kPa.

APPENDIX B

Geometry data for scroll device

```
% Device identification, type, length unit
XXX
scrll
0.001000
% Number of pockets
2
% Table of crank angle, chamber volume, area, moment area
64.000000 19.000000 63.000000 63.000000
0.000000 -0.000000 -419.462929 -15.753380 56.731519 48.758980 -150.064709 318.844946
0.314159 306.993060 -509.189734 -61.471471 80.298972 131.273331 -180.682239 694.108881
0.628319 857.965761 -580.397329 -132.679066 111.490789 250.867538 -182.265935 1089.058356
0.942478 1653.143220 -626.115420 -222.405871 150.314004 397.606619 -129.190222 1465.032965
1.256637 2668.846095 -641.868800 -321.868800 196.028639 545.214453 -0.000000 1785.229693
1.570796 3859.969381 -626.477350 -420.228612 247.066116 652.046029 211.331322 2014.614417
1.884956 5162.844638 -518.722148 -630.153970 320.524383 721.202533 523.969886 2197.366743
2.199115 6576.219219 -336.443740 -811.685465 400.389728 654.537227 900.906153 2376.409481
2.513274 8100.248299 -89.044995 -937.148668 486.507809 418.106425 1286.883873 2555.452220
2.827433 9734.931877 204.908042 -983.171524 578.878628 -0.042123 1610.023054 2734.494959
3.141593 11480.269952 518.588424 -932.954701 677.502184 -582.344408 1792.097128 2913.537697
3.455752 13336.262526 819.343704 -779.119477 782.378476 -1279.099399 1760.426281 3092.580436
3.769911 15302.909597 1072.082794 -525.633474 893.507506 -2010.566971 1460.686776 3271.623175
4.084070 17380.211167 1243.264087 -188.507924 1010.889273 -2674.050970 868.793113 3450.665913
4.398230 19568.167234 1305.040324 204.908042 1134.523777 -3155.526059 -0.045030 3629.708652
4.712389 21866.777799 1239.070120 618.051353 1264.411017 -3344.659968 -1086.777244 3808.751391
5.026548 24276.042862 1039.516807 1008.533438 1400.550995 -3151.475143 -2289.695143 3987.794130
5.340708 26795.962424 714.823208 1332.480123 1542.943710 -2522.476861 -3471.878598 4166.836868
5.654867 29426.536483 287.970853 1549.379507 1691.589162 -1453.920696 -4474.623179 4345.879607
5.969026 32167.765040 -204.908042 1626.909124 1846.487351 -0.042123 -5135.713256 4524.922346
6.283185 17509.821181 -149.025676 780.469460 975.453217 8572.904241 -4373.415420 -8456.767198
6.283185 17509.826913 -149.025676 780.469460 975.453541 -6896.192364 -787.147789 12841.887336
6.597345 18837.593428 -344.266719 680.692803 1047.371322 10206.725237 -1984.001173 -9082.365488
6.597345 18837.599160 -344.266719 680.692803 1047.371646 -6782.247264 -2729.491402 13271.264430
6.911504 20098.703103 -506.240061 518.346004 1118.603614 11145.597539 1050.325730 -9732.383513
6.911504 20098.708835 -506.240061 518.346004 1118.603938 -6111.629855 -4707.792970 13705.375719
7.225663 21293.037648 -614.689753 304.919826 1189.146575 11143.941803 4510.342560 -10422.444315
7.225663 21293.043380 -614.689753 304.919826 1189.146899 -4852.953738 -6554.467208 14198.504651
7.539822 22432.436734 -653.454562 58.480379 1259.370195 10026.344934 8083.999627 -11167.420345
7.539822 22432.442466 -653.454562 58.480379 1259.370518 -3020.980555 -8084.044657 14802.326691
7.853982 23539.533315 -612.592770 -197.822741 1329.981753 7720.875121 11391.069686 -11979.977645
7.853982 23539.378143 -612.230839 -198.925858 1330.136094 -682.925984 -9103.801458 15564.542006
8.168141 24645.923122 -520.794658 -378.379468 1392.663464 4342.154705 14086.893540 -12631.184260
8.168141 24645.923122 -520.794658 -378.379468 1392.663464 1925.162244 -9533.421240 16212.039033
8.482300 25752.468102 -378.379468 -520.794658 1455.190835 23.083679 15754.128968 -13278.681287
8.482300 25752.468102 -378.379468 -520.794658 1455.190835 4734.829001 -9205.423975 16859.536061
8.796459 26859.013081 -198.925858 -612.230839 1517.718205 -4914.740006 16064.688904 -13926.178315
8.796459 26859.013081 -198.925858 -612.230839 1517.718205 7523.603400 -8035.432986 17507.033089
9.110619 27965.558060 -0.000000 -643.737600 1580.245575 -10035.545198 14795.232921 -14573.675342
9.110619 27965.558060 -0.000000 -643.737600 1580.245575 10035.545198 -6004.958884 18154.530116
9.424778 29072.103040 198.925858 -612.230839 1642.772946 -14824.750785 11865.181842 -15221.172370
9.424778 29072.103040 198.925858 -612.230839 1642.772946 12000.926053 -3174.342954 18802.027144
9.738937 30178.648019 378.379468 -520.794658 1705.300316 -18736.535044 7364.006557 -15868.669398
9.738937 30178.648019 378.379468 -520.794658 1705.300316 13160.860839 310.250612 19449.524171
10.053096 31285.192999 520.794658 -378.379468 1767.827687 -21250.698418 1562.437523 -16516.166425
10.053096 31285.192999 520.794658 -378.379468 1767.827687 13295.053204 4217.677063 20097.021199
10.367256 32391.737978 612.230839 -198.925858 1830.355057 -21933.319337 -5095.520539 -17163.663453
10.367256 32391.737978 612.230839 -198.925858 1830.355057 12250.105994 8241.787277 20744.518227
10.681415 33498.282958 643.737600 -0.000000 1892.882427 -20494.675255 -12020.984239 -17811.160480
10.681415 33498.282958 643.737600 -0.000000 1892.882427 9965.327464 12020.984239 21392.015254
10.995574 34604.827937 612.230839 198.925858 1955.409798 -16837.534950 -18527.980397 -18458.657508
10.995574 34604.827937 612.230839 198.925858 1955.409798 6492.738637 15166.752321 22039.512282
11.309734 35711.372917 520.794658 378.379468 2017.937168 -11089.328520 -23897.277500 -19106.154536
11.309734 35711.372917 520.794658 378.379468 2017.937168 2008.131130 17299.401391 22687.009309
11.623893 36817.917896 378.379468 520.794658 2080.464539 -3612.892319 -27450.737978 -19753.651563
11.623893 36817.917896 378.379468 520.794658 2080.464539 -3189.424171 18088.152543 23334.506337
11.938052 37924.462876 198.925858 612.230839 2142.991909 5007.599399 -28628.928483 -20401.148591
11.938052 37924.462876 198.925858 612.230839 2142.991909 -8691.269481 17291.757714 23982.003365
12.252211 39031.007855 0.000000 643.737600 2205.519279 14006.423280 -27063.654465 -21048.645618
12.252211 39031.007855 0.000000 643.737600 2205.519279 -14006.423280 14795.232921 24629.500392
12.566371 40137.552835 -198.925858 612.230839 2268.046650 22499.911680 -22636.866772 -21696.142646
12.566371 40137.552835 -198.925858 612.230839 2268.046650 -18601.280260 10638.113032 25276.997420
12.880530 41244.097814 -378.379468 520.794658 2326.975483 29636.125220 -15597.276537 -22343.639673
12.880530 41244.097814 -378.379468 520.794658 2330.574020 -21949.042895 5029.982982 25924.494447
% Leak number, types, and dimensions
5
1 2 1 2 1
4.495800 -2.000000 4.495800 -4.000000 4.495800
-1.000000 32.000000 -3.000000 32.000000 -5.000000
0.025400 0.025400 0.025400 0.025400 0.025400
15.799698 17.373178 18.946659 20.520139 22.093619
23.667100 27.336149 31.355727 35.690001 40.338970
45.302635 49.007514 53.027090 57.361361 62.010329
66.973992 70.156781 73.303738 76.450696 79.597654
82.744612 0.000000 85.891570 0.000000 89.038529
0.000000 92.185488 0.000000 95.332447 0.000000
98.479406 0.000000 101.626365 0.000000 104.773325
0.000000 107.920284 0.000000 111.067244 0.000000
```

```
114.214204 0.000000 117.361163 0.000000 120.508123
0.000000 123.655083 0.000000 126.802043 0.000000
129.949003 0.000000 133.095963 0.000000 136.242923
0.000000 139.389883 0.000000 142.536843 0.000000
145.683803 0.000000 148.830764 0.000000 3.156298
3.156298 3.156298 3.156298 3.156298 3.156298
26.004371 30.650574 35.660533 41.034248 46.771718
52.872944 59.337926 66.166664 73.359158 80.915408
88.835413 97.119174 105.766692 114.777965 124.152993
0.000000 133.891778 0.000000 143.994318 0.000000
154.460615 0.000000 165.290667 0.000000 176.484475
0.000000 188.042039 0.000000 199.963358 0.000000
212.248434 0.000000 224.897265 0.000000 237.909852
0.000000 251.286195 0.000000 265.026294 0.000000
279.130149 0.000000 293.597759 0.000000 308.429125
0.000000 323.624248 0.000000 339.183126 0.000000
355.105759 0.000000 371.392149 0.000000 388.042295
0.000000 405.056196 0.000000 28.917155 30.490636
32.064116 33.637597 35.211077 36.748751 40.453634
44.473212 48.807485 53.456454 45.302661 49.007541
53.027117 57.361388 62.010355 67.009825 70.156781
73.303738 76.450696 79.597654 0.000000 82.744612
0.000000 85.891570 0.000000 89.038529 0.000000
92.185488 0.000000 95.332447 0.000000 98.479406
0.000000 101.626365 0.000000 104.773325 0.000000
107.920284 0.000000 111.067244 0.000000 114.214204
0.000000 117.361163 0.000000 120.508123 0.000000
123.655083 0.000000 126.802043 0.000000 129.949003
0.000000 133.095963 0.000000 136.242923 0.000000
139.389883 0.000000 142.536843 0.000000 145.683803
0.000000 148.830764 3.156298 3.156298 3.156298
3.156298 3.156298 21.721924 26.004371 30.650574
35.660533 41.034248 46.771718 52.872944 59.337926
66.166664 73.359158 80.915408 88.835413 97.119174
105.766692 114.777965 0.000000 124.152993 0.000000
133.891778 0.000000 143.994318 0.000000 154.460615
0.000000 165.290667 0.000000 176.484475 0.000000
188.042039 0.000000 199.963358 0.000000 212.248434
0.000000 224.897265 0.000000 237.909852 0.000000
251.286195 0.000000 265.026294 0.000000 279.130149
0.000000 293.597759 0.000000 308.429125 0.000000
323.624248 0.000000 339.183126 0.000000 355.105759
0.000000 371.392149 0.000000 388.042295 0.000000
405.056196 0.000000 0.000000 0.000000 0.000000
0.000000 0.000000 0.000000 0.000000 0.000000
0.000000 0.000000 0.000000 0.000000 0.000000
0.000000 0.000000 0.000000 0.000000 0.000000
0.000000 13.703239 0.000000 17.408119 0.000000
21.427694 0.000000 25.761966 0.000000 30.410933
0.000000 35.374596 0.000000 38.557386 0.000000
41.704343 0.000000 44.851300 0.000000 47.998258
0.000000 51.145216 0.000000 54.292175 0.000000
57.439134 0.000000 60.586092 0.000000 63.733051
0.000000 66.880011 0.000000 70.026970 0.000000
73.173929 0.000000 76.320889 0.000000 79.467848
0.000000 82.614808 0.000000 85.761768 0.000000
% Leak path
22 21 21 22 0
24 23 23 24 0
26 25 25 26 0
28 27 27 28 0
30 29 29 30 0
32 31 31 32 0
34 33 33 34 0
36 35 35 36 0
38 37 37 38 0
40 39 39 40 0
42 41 41 42 0
44 43 43 44 0
46 45 45 46 0
48 47 47 48 0
50 49 49 50 0
52 51 51 52 0
54 53 53 54 0
56 55 55 56 0
58 57 57 58 0
60 59 59 60 0
62 61 0 0 22
0 0 61 62 0
64 63 0 0 24
0 0 63 64 0
66 65 0 0 26
0 0 65 66 0
68 67 0 0 28
0 0 67 68 0
70 69 0 0 30
0 0 69 70 0
72 71 0 0 32
0 0 71 72 0
74 73 0 0 34
0 0 73 74 0
76 75 0 0 36
0 0 75 76 0
78 77 0 0 38
0 0 77 78 0
```

```
80 79 0 0 40
0 0 79 80 0
82 81 0 0 42
0 0 81 82 0
84 83 0 0 44
0 0 83 84 0
86 85 0 0 46
0 0 85 86 0
88 87 0 0 48
0 0 87 88 0
90 89 0 0 50
0 0 89 90 0
92 91 0 0 52
0 0 91 92 0
94 93 0 0 54
0 0 93 94 0
96 95 0 0 56
0 0 95 96 0
98 97 0 0 58
0 0 97 98 0
100 99 0 0 60
0 0 99 100 0
102 101 0 0 62
0 0 101 102 0
104 103 0 0 64
0 0 103 104 0
```

REFERENCES AND LITERATURE

Adair R. P., Qvale E. B., Pearson J. T. 1972: Instantaneous Heat Transfer to the Cylinder Wall in Reciprocating Compressors, Proc. of the Int. Compressor Conf. Purdue, West Lafayette, IL, USA, 1972

Adiprasito B.., 2000: CO_2-A/C-system COP comparison R134a vs. CO_2, SAE Alternate Refrigerant Systems Symposium, Phoenix, 2000

Alefeld G., Radermacher R., 1994: Heat Conversion Systems, CRC Press, Boca Raton, Ann Arbor, 1994

ARI 1999: Standard for positive displacement refrigerant compressors and compressor units, Standard 540, 1999

ARI 2002: R-22 Alternative Refrigerants Evaluation Program (AREP), http://www.ari.org/rt/arep/intro.html

ASHRAE 1998: Handbook, Refrigeration

Baek J. S., Groll E. A., Lawless P. B., 2002: Development of a Piston-Cylinder Expansion Device for the Transcritical Carbon Dioxide Cycle, Proceedings of the International Refrigeration Conference at Purdue, West Lafayette, IN, 2002

Bejan A., 1997: Advanced Engineering Thermodynamics, John Wiley & Sons Inc, New York, Chichester, 1997

Bhatti M. S., 1997: A Critical Look at R744 and R134a Mobile Air-Conditioning Systems, SAE International Congress & Exposition, Detroit, MI, 1997

Bodenius, W.S., 1999: The Rise and Fall of Carbon Dioxide Systems, ASHRAE Journal, Atlanta, April 1999

Brok S. W., Touber S., van der Meer J. S., 1980: Modeling of Cylinder Heat transfer – Large Effort, Little Effect? Proceedings of the International Compressor Conference at Purdue, West Lafayette, IN, 1980

Bullard C. W., Yin J. M., Hrnjak P. S., 2000: Transcritical CO_2 Mobile Heat Pump And A/C System, Experimental And Model Results, SAE Alternate Refrigerant Systems Symposium, Phoenix, 2000

Caillat J. L., Shimona N., Daniels M., 1988: A Computer Model for Scroll Compressors, Proceedings of the International. Compressor Conference Purdue, West Lafayette, IL, USA, 1988

CITY 2002: The Expressor, http://www.staff.city.ac.uk/~sj376/expr.htm

Cuttler B. J, 2000: Development of a Carbon Dioxide Environmental Control Unit, Master thesis at the University of Maryland College Park, 2000

Fischer S. K., 1993: Total Equivalent Warming Impact: A Measure Of The Global Warming Impact Of CFC Alternatives In Refrigerating Equipment, International Journal of Refrigeration, v16 n6, 1993

Fukuta M., Yanagisawa T., Ogi Y., Radermacher R., 2001: Cycle Performance of CO_2 Cycle with Vane Compressor-Expander Combination, ImechE pp. 315-324, 2001

Fukuta M., Lee B. C., Yanagisawa T., Choi S., 2002: A Study on the Leakage Characteristics of Tip Seal Mechanism in the Scroll Compressor, Proceedings of the International Compressor Conference at Purdue, West Lafayette, IN, 2002

Gerwen R.J.M, Koffijberg H., 1995: Natural Refrigerants: Applications and Risks, 19th International Congress of Refrigeration Proceedings 4b, IIR B2, 1995

Hafner A., Pettersen J., Skaugen G., Neksa P., 1998: An Automobile HVAC System with CO_2 as the Refrigerant, IIF-IIR - Section B and E, Oslo, Norway, 1998

Halozan, H, Rieberer, R, 1999: Heat Pumps in Low-Heating-Energy Buildings, IIR International Congress of Refrigeration '99, Sydney, Australia, Paper 499, 1999

Hartmann K., 1994: Keisverbesserung durch Entspannungsturbine, KI Luft- und Kaeltetechnik, pp. 421-424, September 1994

Hauk A., Weidner E., 2000: Thermodynamic and Fluid-Dynamic Properties of CO_2 with Different Lubricants in Cooling Circuits for Automobile Applications, Ind. Eng. Chem. Res., v39, pp. 4646-4651, 2000

Heidelck R., Kruse H., 2000: Expansion Machines for CO_2 Based on Modified Reciprocating Machines, IFF-IIR-Commission B1, B2, E1 and E2, Purdue University, USA, 2000

Heyl P., 2000: Untersuchung transkritischer CO_2 Prozesse mit arbeitsleistender Entspannung; Prozessberechnung, Auslegung und Test einer Expansions-KompressionsMaschine, Forschungsberichte des DKV, Nr. 62, DKV, 2000

Heyl P., Quack H., 2000: Transcritical CO_2-Cycle with Expander-Compressor, Proceedings of the International Refrigeration Conference at Purdue, West Lafayette, IN, 2000

Hirao T., Mizukami H., Takeuchi M., Taniguchi M., 2000: Development of Air-Conditioning System Using CO_2 for Automobile, 4th IIR-Gustav Lorentzen Conference on Natural Working Fluids at Purdue, West Lafayette, IN, pp.199-206, 2000

Horst L., 1911: Verbesserte CO_2-Expansions-Kaeltemaschine, Zeitschrift fuer Sauerstoff- und Stickstoff-Industrie, Heft 12, 1911

Huff H.-J., Hwang Y., Radermacher R., 2002: Options for a Two-Stage Transcritical Carbon Dioxide Cycle, Proceedings of IIR-Gustav Lorentzen Conference on Natural Working Fluids, Guangzhou, China, 2002

Hwang Y., Radermacher R., 1998: Total Equivalent Warming Impact Analysis Of Automotive Air-Conditioning, EPA Project, prepared by University of Maryland, College Park, December 1998

Hwang Y., Radermacher R., 1998a: Experimental Evaluation of CO_2 Water Heater, Proceedings of IIR-Gustav Lorentzen Conference, Natural Working Fluids, Oslo, Norway, 1998

Ijima K., 2000: A CO_2 Refrigerant System for Vehicle Air Conditioning, SAE Alternate Refrigerant Systems Symposium, Phoenix, 2000

Ishii, N., Bird, K., Sano, K., Mamoru, O. Iwamura, S., Otokura, T., 1996: “Refrigerant Leakage Flow Evaluation for Scroll Compressors”, Proceedings of the Purdue Compressor Technology Conference, West Lafayette, IN, USA, pp. 633 – 638, 1996

Koehler J., Sonnekalb M., 1998b: A Transcritical Refrigeration Cycle with Carbon Dioxide for Bus Air-Conditioning and Transportation Refrigeration, Proceedings of the International Refrigeration Conference at Purdue, West Lafayette, IN, 1998

Koehler J., Sonnekalb M., Kaiser H., 1998a: A Transcritical Refrigeration Cycle with Carbon Dioxide for Bus Air-Conditioning and Transportation Refrigeration, Proceedings of IIR-Gustav Lorentzen Conference, Natural Working Fluids, Oslo,

Norway, 1998
Koehler J., Sonnekalb M., Lehmke N., 1999: Second Year of City Busses with Transcritical Air-Conditioning Units in Germany, SAE Alternate Refrigerant Systems Symposium, Phoenix, 1999
Koehler J., Sonnekalb, M., 1996: CO_2 als Kältemittel in Omnibus-Klimaanlagen, Proceedings of the Conference: Fahrzeugklimatisierung mit natürlichen Kältemitteln, Johannes Reichelt, Hrsg., 1996
Lee G. H., Kim G. W., 2001: Performance Simulation of Scroll Compressors, IMechE C591, May 2001
Lin Z. H., 1982: Two-Phase Measurements with Sharp-Edged Orifices, International Journal of Multiphase Flow, v8, n8, pp. 693-693, 1982
Lindsay D, Radermacher R., 2000: Theory and Application of Alternative Scroll Geometries, Proceedings of the Purdue Compressor Technology Conference, West Lafayette, IN, USA, pp. 699-706, 2000
Liu, Z., Soedel, W., 1992: Modeling Temperatures in High Speed Compressors for the Purpose of Gas Pulsation and Valve Loss Modeling, Proceedings of the Purdue Compressor Technology Conference, West Lafayette, IN, USA, pp. 1377-1384, 1992
Lorentzen G., 1994: Revival of Carbon Dioxide as Refrigerant, International Journal of Refrigeration, v17, n5, pp. 292-301, 1994
Lorentzen G., Pettersen J., 1993: A New, Efficient And Environmentally Benign System For Car Air-Conditioning, International Journal of Refrigeration, v16 n1, pp. 4-12, 1993
Maurer T., Zinn T., 2000: Experimentelle Untersuchung von Entspannungsmaschinen mit mechanischer Leistungsauskopploung fuer die transkritische CO_2-Kaeltemaschine, DKV Tagungsbericht Berlin, v26 nII.1, pp. 304-318, 1999
McEnaney R. P., Boewe D. E., Yin J. M., Park Y. C., Bullard C. W., Hrnjak P. S., 1998: Experimental Comparison of Mobile AIC Systems When Operated With Transcritical CO_2 Versus Conventional R134a, Proceedings of the International Refrigeration Conference at Purdue, West Lafayette, IN, 1998
Neksa P., Rekstad H., Zakeri R., Schiefloe P. A. 1998: CO_2-Heat Pump Water Heater: Characteristics, System Design and Experimental Results, International Journal of Refrigeration, v 21 n3, 1998
Neksa P., Dorin F., Rekstad H., Bredesen A. E., Serbisse A., 1999: Development of semi-hermetic CO_2-compressors, 20th International Congress of Refrigeration IIR/IIF, Sidney, 1999
Nippon Soken, Denso Corporation, 1997: Pointing to the Future: Two-Stage CO_2 Compression, Heat Transfer Issues in 'Natural' Refrigerants, University of Maryland, College Park, MD, 1997
Petitjean C., 1999: TEWI Comparison of Current and Future HFC-134a Systems and CO_2, SAE Alternate Refrigerant Systems Symposium, Phoenix, 1999
Plank R., 1912: Verbesserung der Kohlensaeure-Kaeltemaschine durch Einfuehrung eines Expansionszylinders, Zeitschrift fuer die gesamt Kaelteindustrie, Heft 12, 1912
Preissner M., 2001: Carbon Dioxide Vapor Compression Cycle Improvements with Focus on Scroll Expanders, Ph.D. Thesis, University of Maryland, College Park,

2001
Preissner M., Cutler B., Radermacher R., 2000b: Suction Line Heat Exchanger for R134a, Automotive Air-Conditioning System, Proceedings of the International Refrigeration Conference at Purdue, West Lafayette, IN, 2000
Preissner M., Cutler B., Singanamalla S., Hwang Y., Radermacher R., 2000a: Comparison of Automotive Air-Conditioning Systems Operating with CO_2 and R134a, 4th IIR-Gustav Lorentzen Conference on Natural Working Fluids at Purdue, West Lafayette, IN, pp. 191-198, 2000
Preissner M., Huff H.-J., Radermacher R., 2000: Evaporatively Cooled Heat Exchanger, Refrigerant Alternative Consortium, Project Report, 2000
Rieberer, R., Halozan, H. 1998: CO_2 - Heat pump Water Heater: Simulation and Test Results, IIR Conference Proceedings, Purdue ,1998
Rieberer, R., Neksa, P., Schiefloe, P.A., 1999: CO_2 Heat Pumps for Space Heating and Tap Water Heating, IIR International Congress of Refrigeration '99, Sydney, Autralia, Paper 305, 1999
Robinson D. M., Groll E. A., 1996: Using Carbon Dioxide in Transcritical Vapor Compression Refrigeration Cycles, Proceedings of the International Refrigeration Conference at Purdue, West Lafayette, IN, 1996
Robinson D. M., Groll E. A., 1998: Efficiencies of Transcritical CO_2-Cycles with and without an Expansion Turbine, International Journal of Refrigeration, v21,n7, pp. 577 – 589, 1998
Rowland F., Molina M. 1974: Stratospheric Ozone Destruction Catalyzed By Chlorine Atoms From Photolysis Of Chlorofluoromethanes, Transactions, American Geophysical Union, v55 n12, pp. 1153-1153, 1974
Saikawa M. K., Hashimoto K., Hasegawa H., 1997: A Basic Study on CO_2 Heat Pumps Especially for Hot Tap Water Supply, Proceedings of IIR Workshop on CO_2 Technology in Refrigeration and Air-Conditioning Systems, Trondheim, Norway, 1997
Sakamoto S., Giese P., 2000: Sanden/LuK Cooperation on CO_2 Compressors, SAE Alternate Refrigerant Systems Symposium, Phoenix, 2000
Shaw D. N., 1988: Screw Compressors Control of Vi and Capacity "The Conflict," Proceedings of the International Refrigeration Conference at Purdue, West Lafayette, IN, 1988
Shiva Prasad, B. G., 1998: "Heat Transfer in Reciprocating Compressors – A Review", Proceedings of the Purdue Compressor Technology Conference, West Lafayette, IN, USA, pp. 857-863, 1998
Smith I.K., Stosic N., 1995: Expressor: An efficiency boost to vapor compression systems by power recovery from the throttling process, Proceedings of the 1995 ASME International Mechanical Engineering Congress and Exposition, San Francisco, CA, USA, pp. 173-181, 1995
Stosic N., Smith I. K., Kovacevic A., 2002: A Twin Screw Combined Compressor and Expander for CO_2 Refrigeration Systems, Presentation given at the International Refrigeration Conference at Purdue, West Lafayette, IN, 2002
Sumantran V., Khalighi B., Saka K., Fischer S., 1999: An Assessment of Alternative Refrigerants for Automotive Applications Based on Environmental Impact, SAE Alternate Refrigerant Systems Symposium, Phoenix, 1999

Tang Y., Fleming J. S., 1992: Obtaining the Optimum Geometrical Parameters of a Refrigeration Helical Screw Compressor, Presentation given at the International Refrigeration Conference at Purdue, West Lafayette, IN, 1992

Takahashi T., 2000: Development of Carbon Dioxide (CO_2) Applied Refrigeration System Refrigeration System, SAE Alternate Refrigerant Systems Symposium, Phoenix, 2000

Thiessen, H., 1998: Historische Entwicklung, Kohlendioxid – Besonderheiten und Einsatzchancen als Kaeltemittel, Statusbericht des Deutschen Kaelte- und Klimatechnischen Verines, Nr. 20, DKV, pp. 9 – 13, 1998

UNEP 2002a: http://www.unep.ch/ozone/vienna.shtml

UNEP 2002b: The Montreal Protocol on Substances that Deplete the Ozone Layer, UNEP Ozone Secretariat United Nations Environment Programme, Nairobi, 2000

UNEP 2002c: http://www.unep.ch/ozone/ratif.shtml

Wertenbach J., Caesar R., 1998: An Environmental Evaluation of an Automobile Air-Conditioning System with CO_2 versus HFC-134a as Refrigerant, Proceedings of IIR-Gustav Lorentzen Conference, Natural Working Fluids, Oslo, Norway, 1998

White F. M., 1994: Fluid Mechanics, McGraw-Hill Book Company, New York, St. Luis, San Francisco, 1994

Wobst E., 1998: Historische Entwicklung, Kohlendioxid – Besonderheiten und Einsatzchancen als Kaeltemittel, Statusbericht des Deutschen Kaelte- und Klimatechnischen Verines, Nr. 20, DKV, pp. 6-8, 1998

Zhang Z., Qu T., Yu Y., 1998: The Study of Using Carbon Dioxide as the Alternative of R502 in Industrial Refrigeration Applications, Proceedings of the International Refrigeration Conference at Purdue, West Lafayette, IN, 1998